Auger-Meitner effect and its applications

SCE-PES Summer school

Physicum, Tartu

Dr. Marta Berholts

RESEARCHER

UNIVERSITY OF TARTU

29.07.2026

Outline: from fundamentals to applications

- **Auger-Meitner effect**
  - Fundamental mechanism

- **Applications**
  - Surface analysis: Auger Electron Spectroscopy (AES)
  - High-resolution imaging: Auger Electron Microscopy (AEM)
  - Auger-Meitner effect in cancer therapy

Core hole in an atom

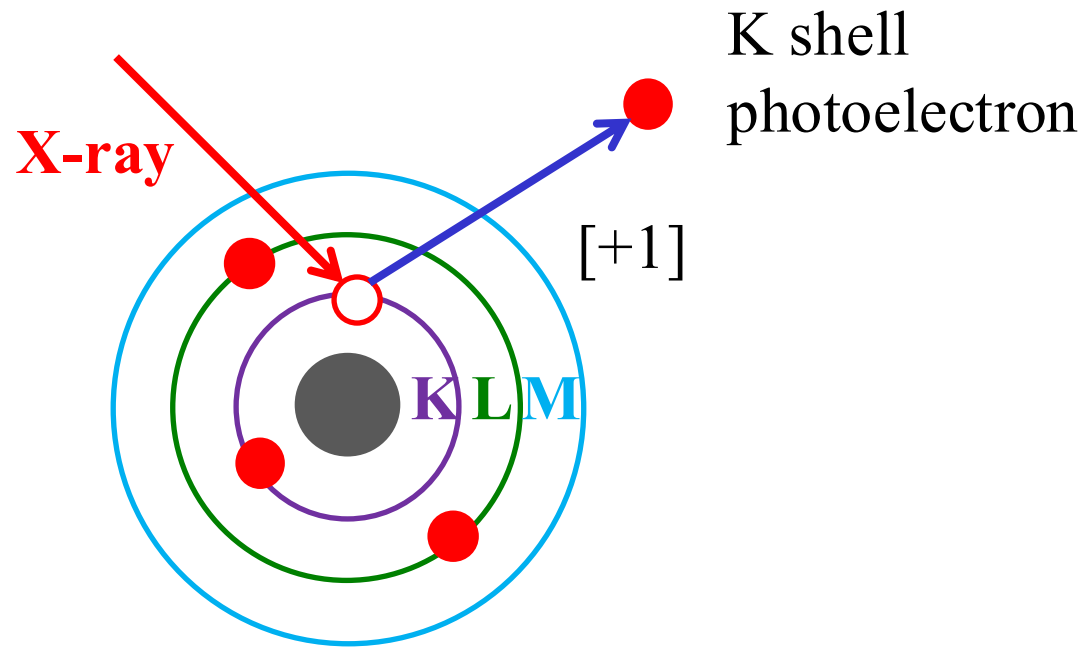

Relaxation
in a few fs

Fluorescence
(radiative)

Auger-Meitner emission
(nonradiative)

The Auger-Meitner effect

Lise Meitner (1878-1968)

First discovered the effect in 1922 while investigating β-ray spectra from radioactive substances

L. Meitner, Z. Phys. 9, 131–144 (**1922**).
L. Meitner, Z. Phys. 17 (**1923**) 54.

Pierre Auger (1899-1993)

Discovered the effect in 1923 and described it in great detail by observing electron tracks in a Wilson cloud chamber (his PhD work)

P. Auger, C.R.A.S. 177 **(1923)** 169 – 171.
P. Auger, Journal de Physique et Le Radium, 6, 205-208 **(1925)**

The Auger-Meitner process

Initial vacancy can be created by:

- Electron/ photon/ ion impact ionization or excitation
- Nuclear processes (internal conversion, electron capture by the nucleus)

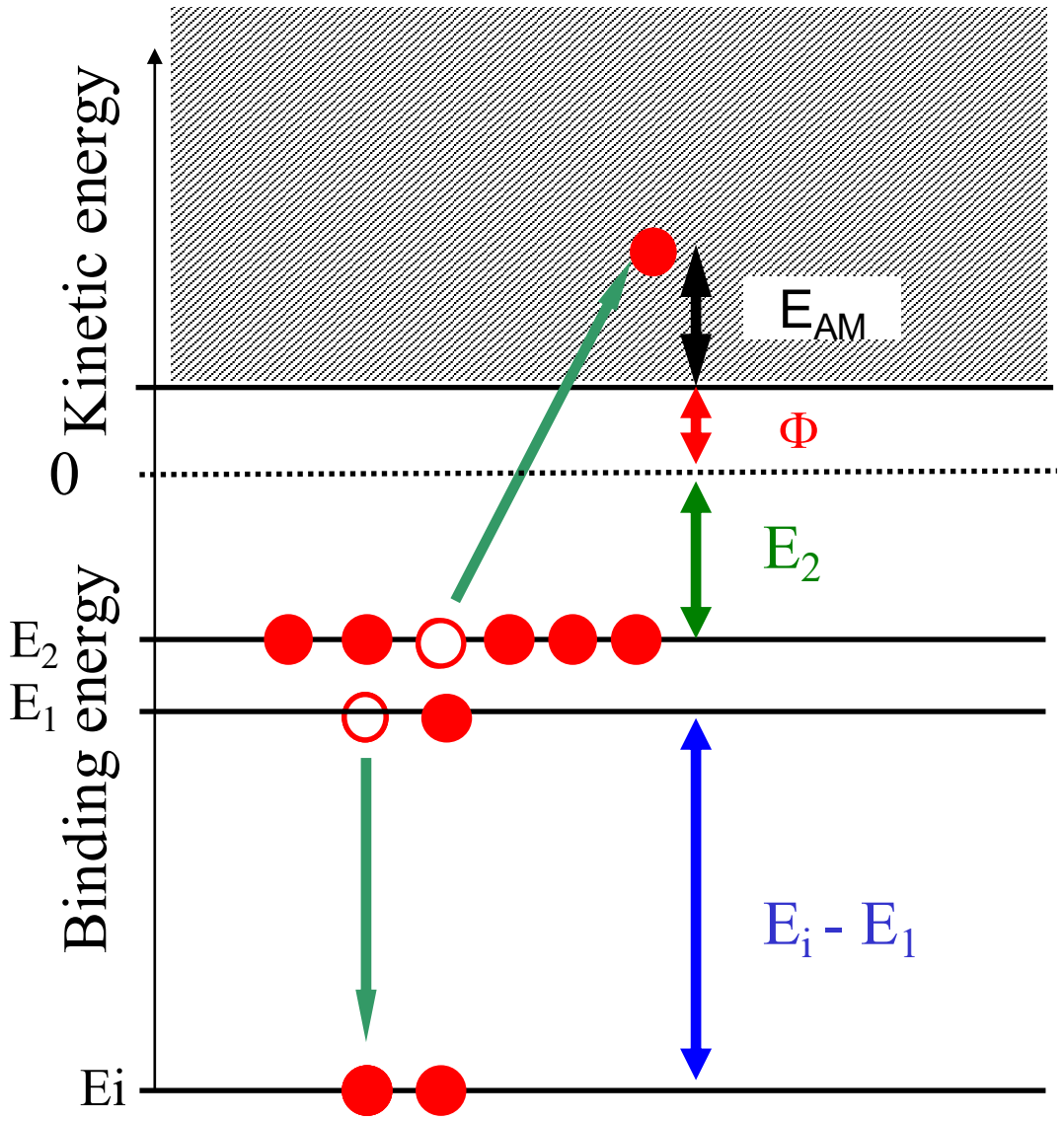

Conservation of energy dictates:

$$E_i - E_1 = E_2 + \Phi + E_{AM}$$

Auger-Meitner electron energy (crude approximation):

$$E_{AM} = E_i - E_1 - E_2 - \Phi$$

- $E_i - E_1$: BE of the shell with initial vacancy
- E_2: BE of the shell from which AM e- is emitted
- Φ: BE of the e- that fills the vacancy

A single Auger-Meitner transition is a three-step process

1. Ionization

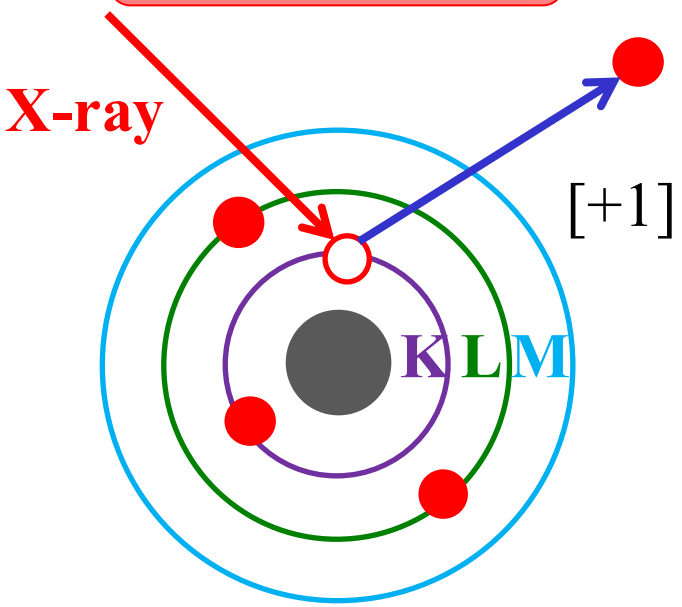

KE = hv - BE

Photoemission
A photoelectron is ejected from an inner shell and a vacancy is created

2. Relaxation

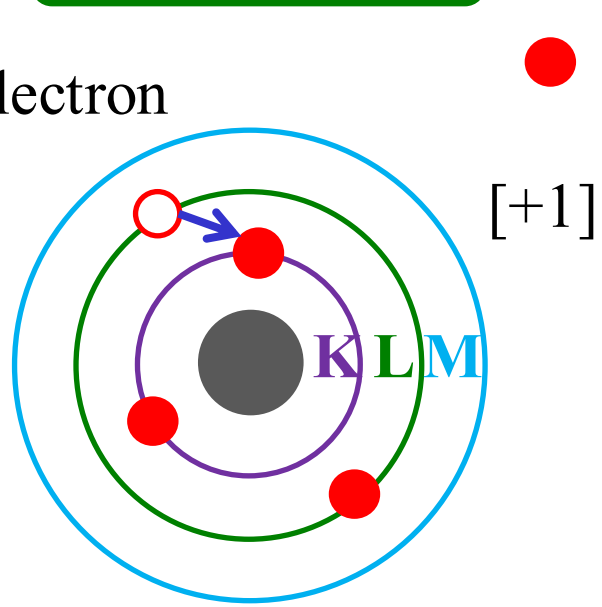

Radiationless relaxation
Higher shell electron fills the vacancy (L->K)

3. Emission

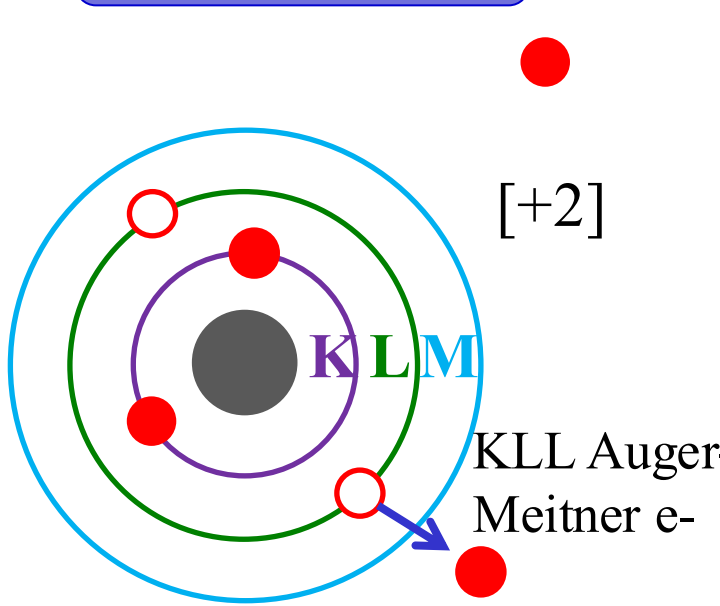

$KE = BE_K - 2BE_L$

Auger-Meitner emission
Released energy ejects secondary electron

The Auger-Meitner transitions are named using X-ray notation

Quantum Numbers			Level Symbol	Auger Notation	XPS Notation
n	ℓ	j			
1	0	1/2	$^2S_{½}$	K	$1s_{1/2}$
2	0	1/2	$^2S_{½}$	L_1	$2s_{1/2}$
2	1	1/2	$^2P_{½}$	L_2	$2p_{1/2}$
2	1	3/2	$^2P_{3/2}$	L_3	$2p_{3/2}$
3	0	1/2	$^2S_{½}$	M_1	$3s_{1/2}$
3	1	1/2	$^2P_{½}$	M_2	$3p_{1/2}$
3	1	3/2	$^2P_{3/2}$	M_3	$3p_{3/2}$
3	2	3/2	$^2D_{3/2}$	M_4	$3d_{3/2}$
3	2	5/2	$^2D_{5/2}$	M_5	$3d_{5/2}$

When a valence electron is involved, the letter V is often used (e.g., **KLV, KVV, LMV**)

The strongest transitions are of the type ABB (e.g., **KLL, LMM**)

Coster-Kronig transitions (1935) are also very strong (**AAB**) and super Coster-Kronig (**AAA**)

Coster-Kronig and super Coster-Kronig transitions

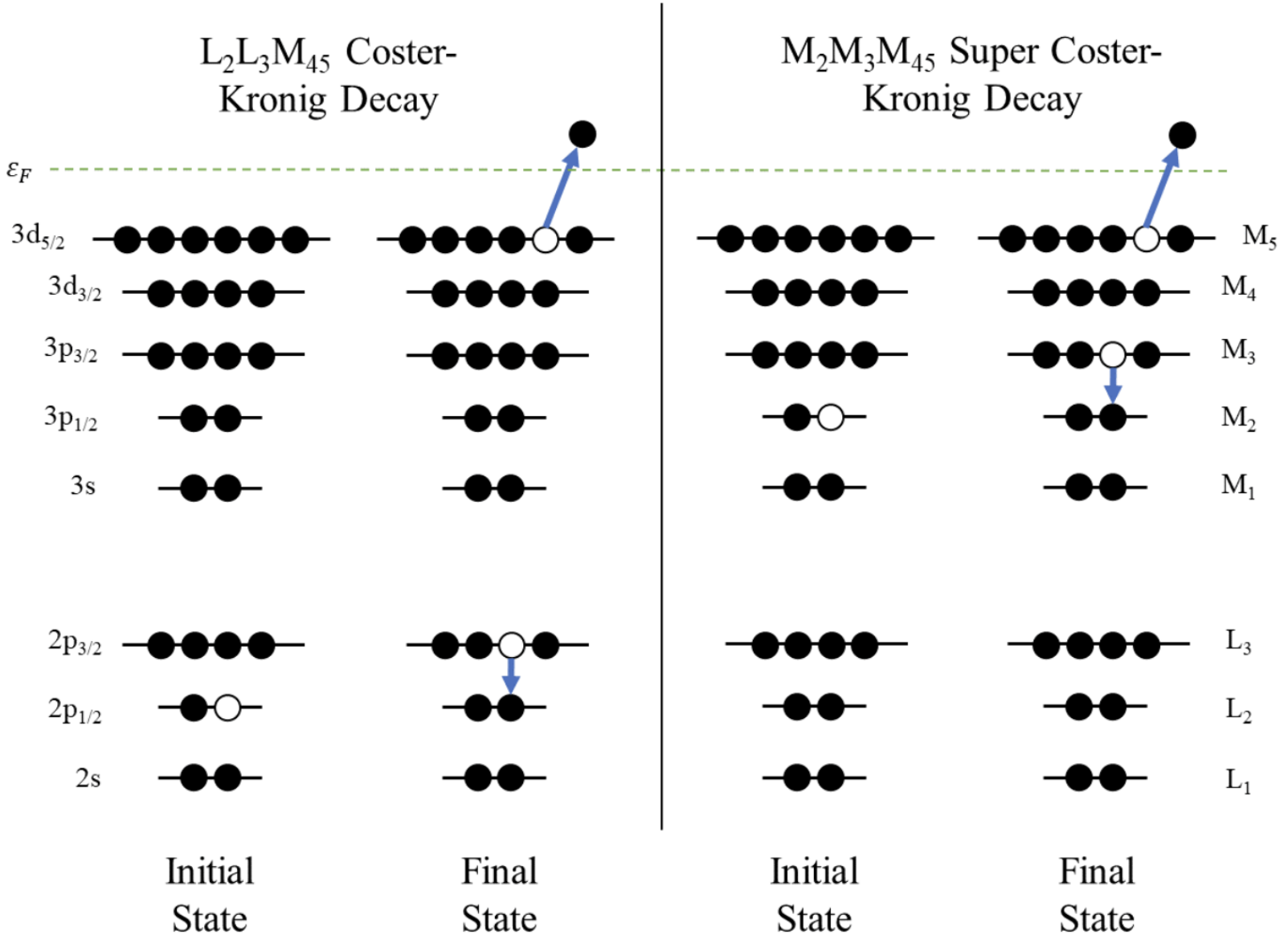

Competition between Auger-Meitner decay and X-ray fluorescence

The sum of the Auger-Meitner yield and X-ray emission yield is unity

Auger-Meitner decay probability:

$$W_A = 1 - \frac{1}{1 + aZ^{-4}},$$

Where Z – atomic number

a – constant

Z < 30 → Auger decay dominates

Z > 30 for K shells and **Z > 92** for L-shells → X-ray fluorescence dominates

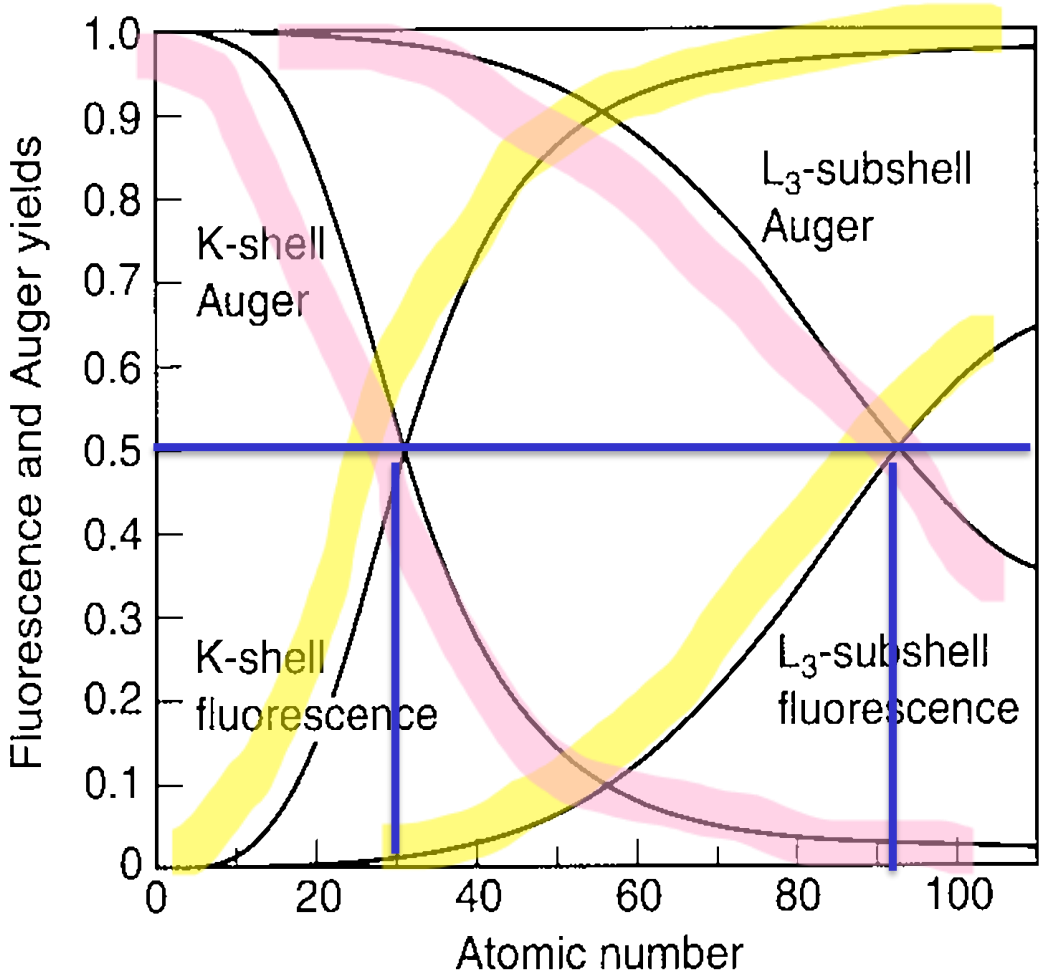

The Auger-Meitner peaks in an electron spectrum

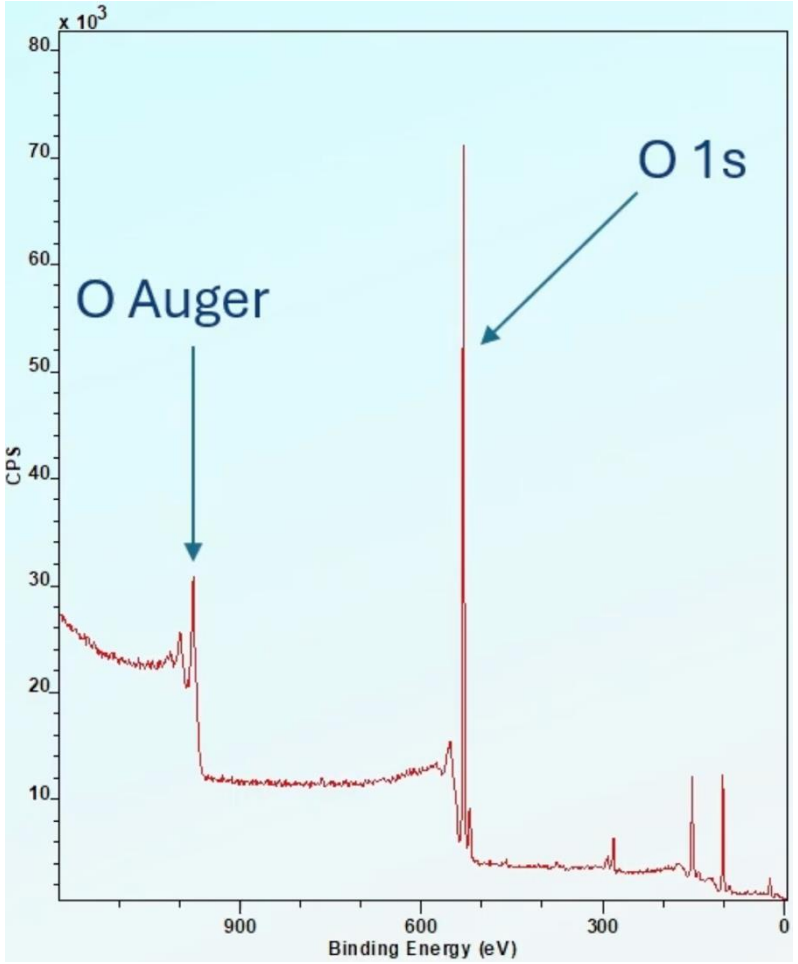

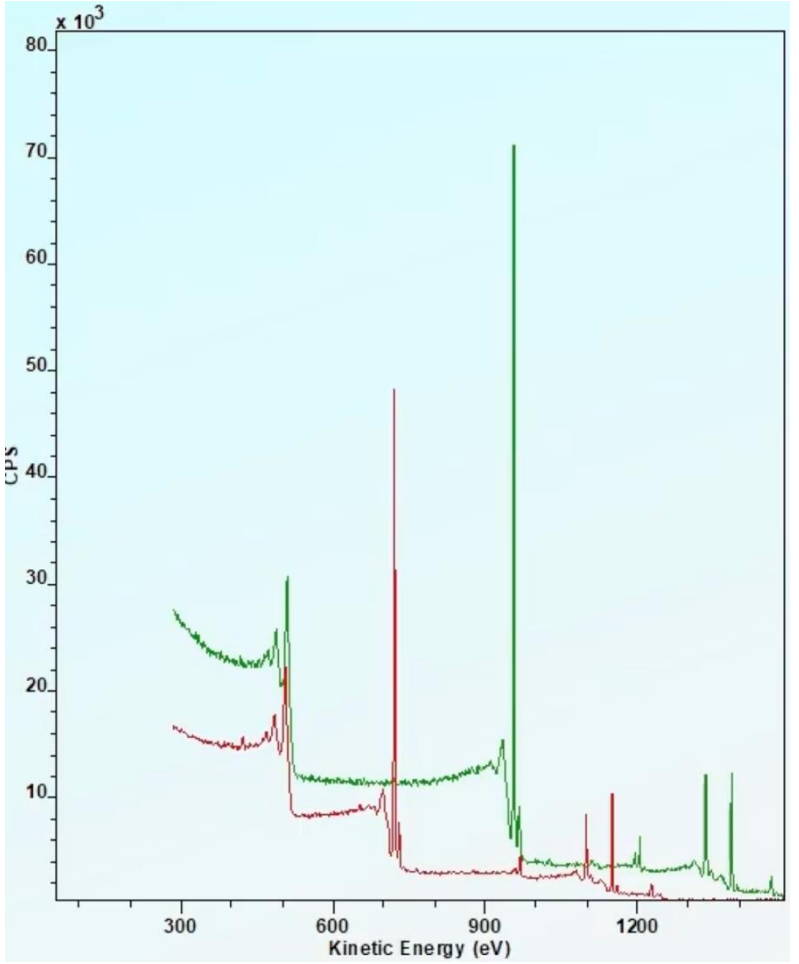

https://www.youtube.com/watch?v=qjzx1UX9B_Y

Auger electrons and photoelectrons in a spectrum

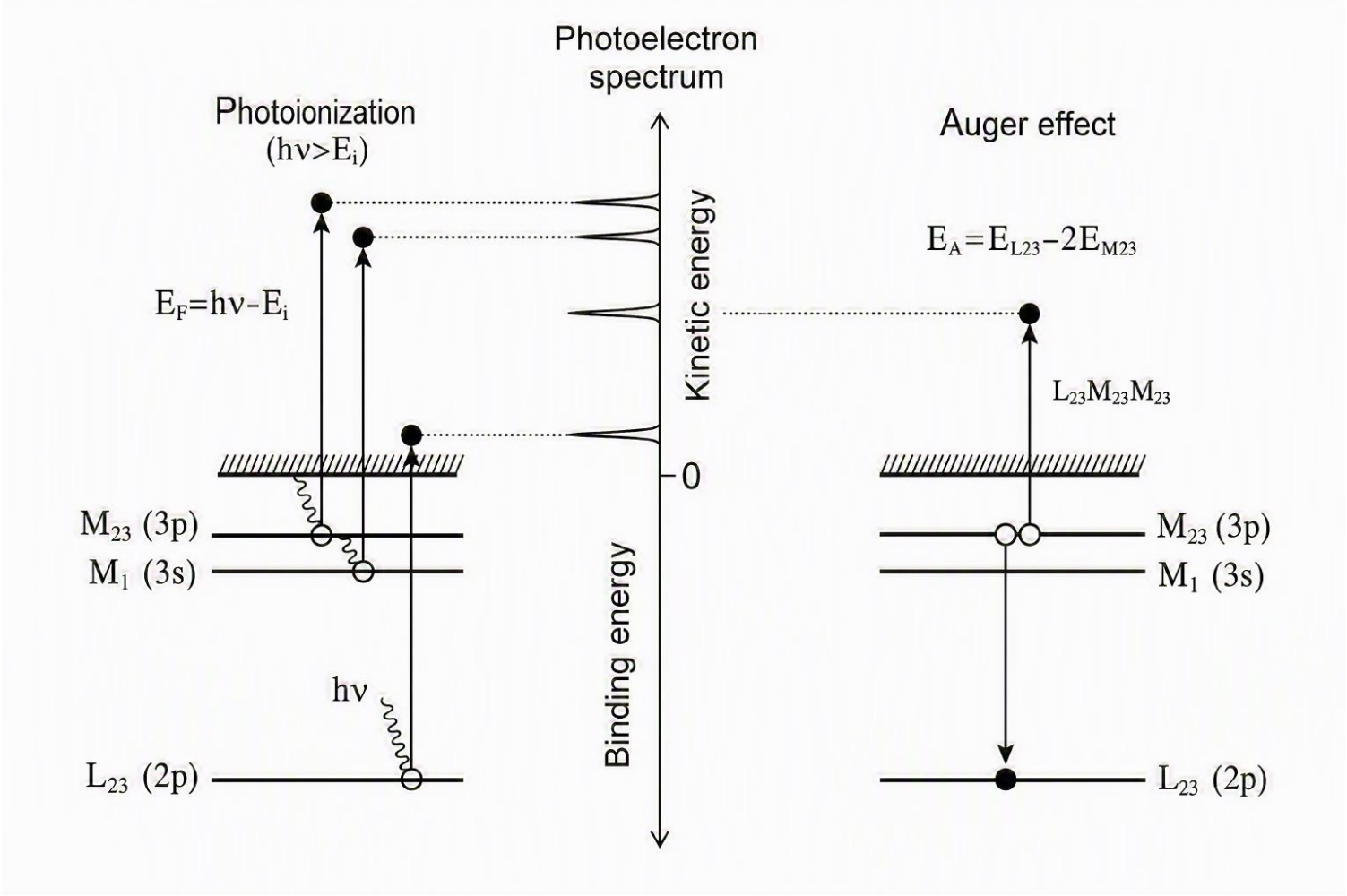

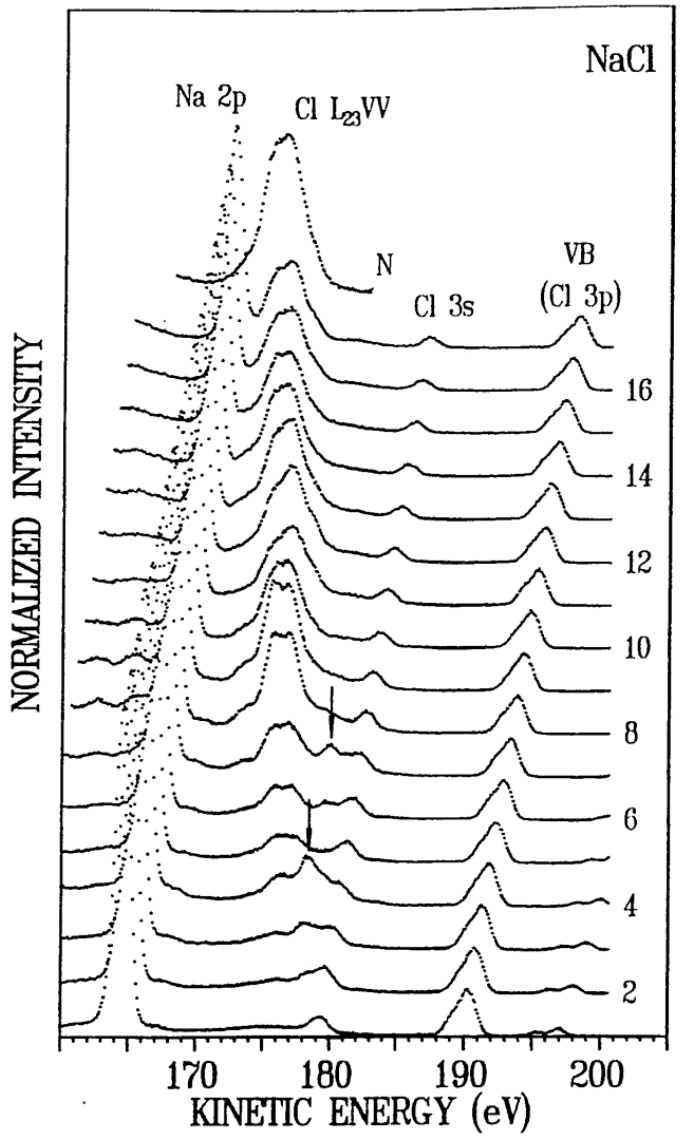

When monochromatic photons are used for ionization:

- photoelectron peaks appear at constant **binding** energies
- Auger peaks appear at constant **kinetic** energies

Resolution of different analyzers

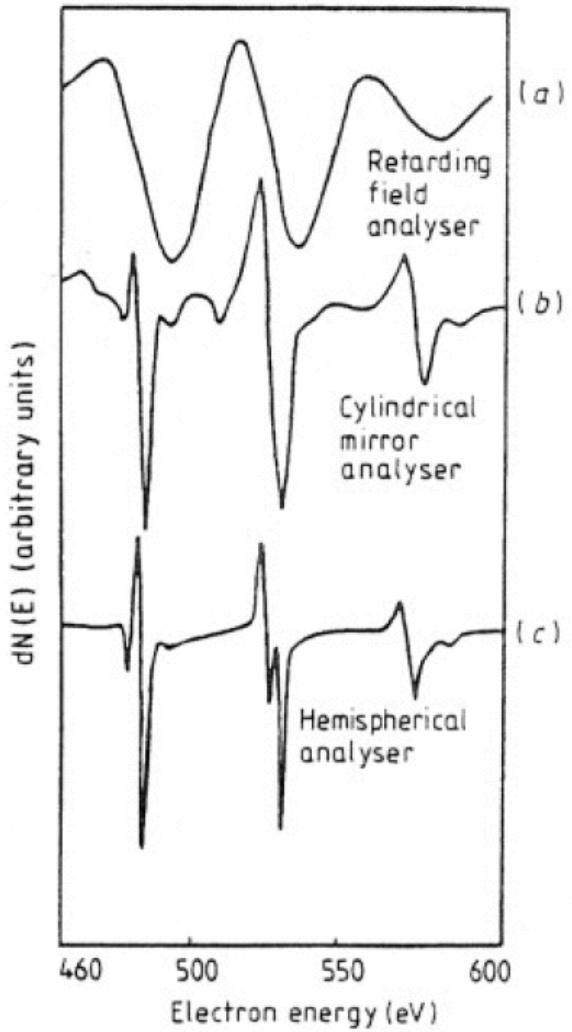

Spectra of metallic Cr measured using different electron energy analyzers:

(a) Retarding field analyzer;
(b) Cylindrical mirror analyzer;
(c) Hemispherical analyzer.

Figure 6.114. Energy resolution with different types of Auger analysers: (a) retarding field, (b) cylindrical mirror and (c) hemispherical (Wild (1981)) (reproduced with permission of Pergamon Press).

Principal Auger electron energies for each element

- Three Auger series dominate most spectra: KLL, LMM, and MNN.

- Each element has characteristic Auger-Meitner electron energies, depending on the electronic structure of the atom → surface and chemical analysis is possible (AES, AEM)

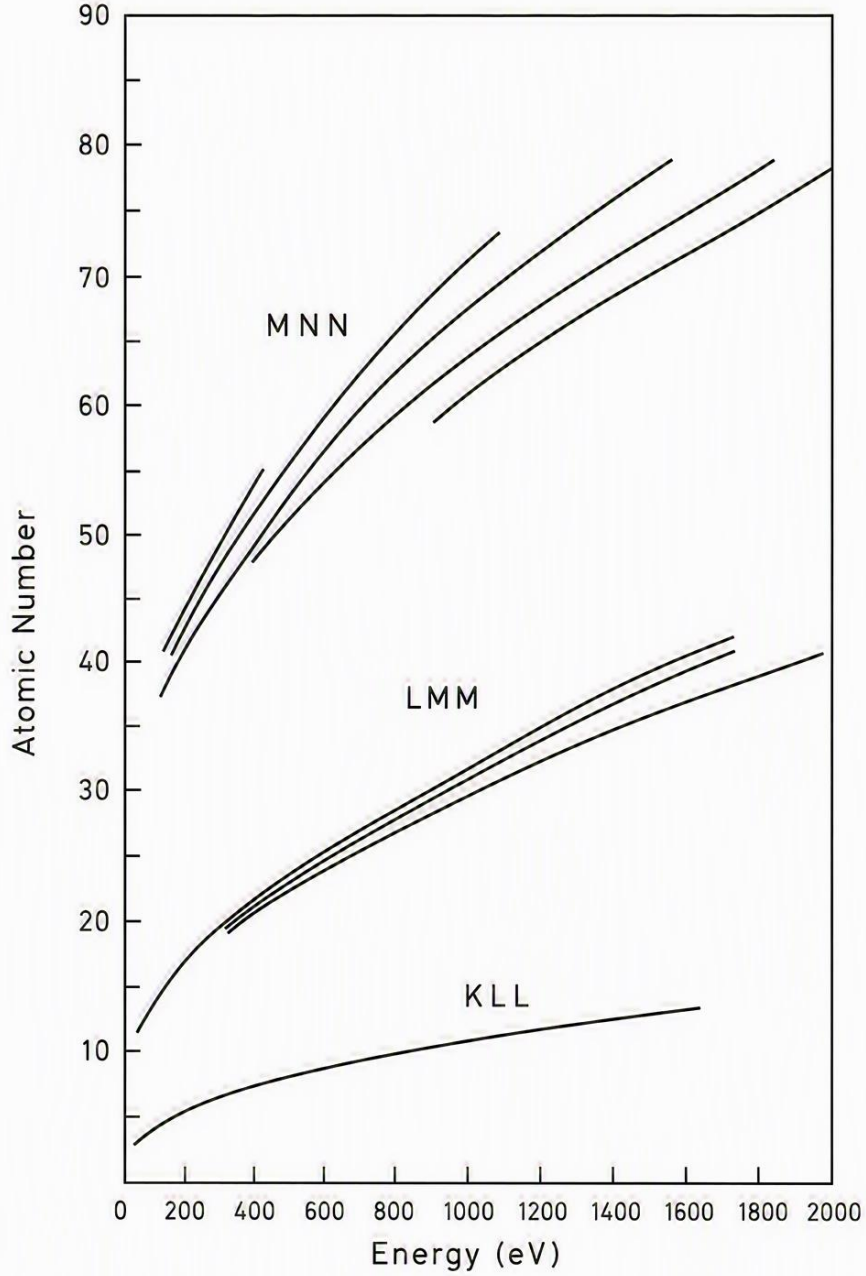

Figure 6.113. Energies of Auger peaks.

The Auger-Meitner cascade

A single core vacancy can trigger a cascade of sequential radiationless and radiative transitions. In heavy atoms such as Xe, this process can generate highly charged ions.

Experiments with Xe have observed average charge states around **+8** and maximum charge state **+22** following K-shell ionization.

NB! Radiative transitions can also participate in a cascade.

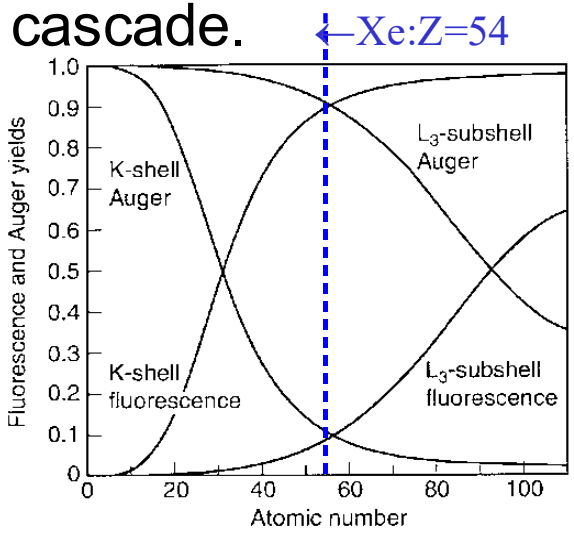

Xe K (1s): BE 34561 eV
Xe L_3 ($2p_{3/2}$): BE 4782 eV

Xe K (1s) 90% fluorescence
Xe L_3 ($2p_{3/2}$): 90% Auger decay

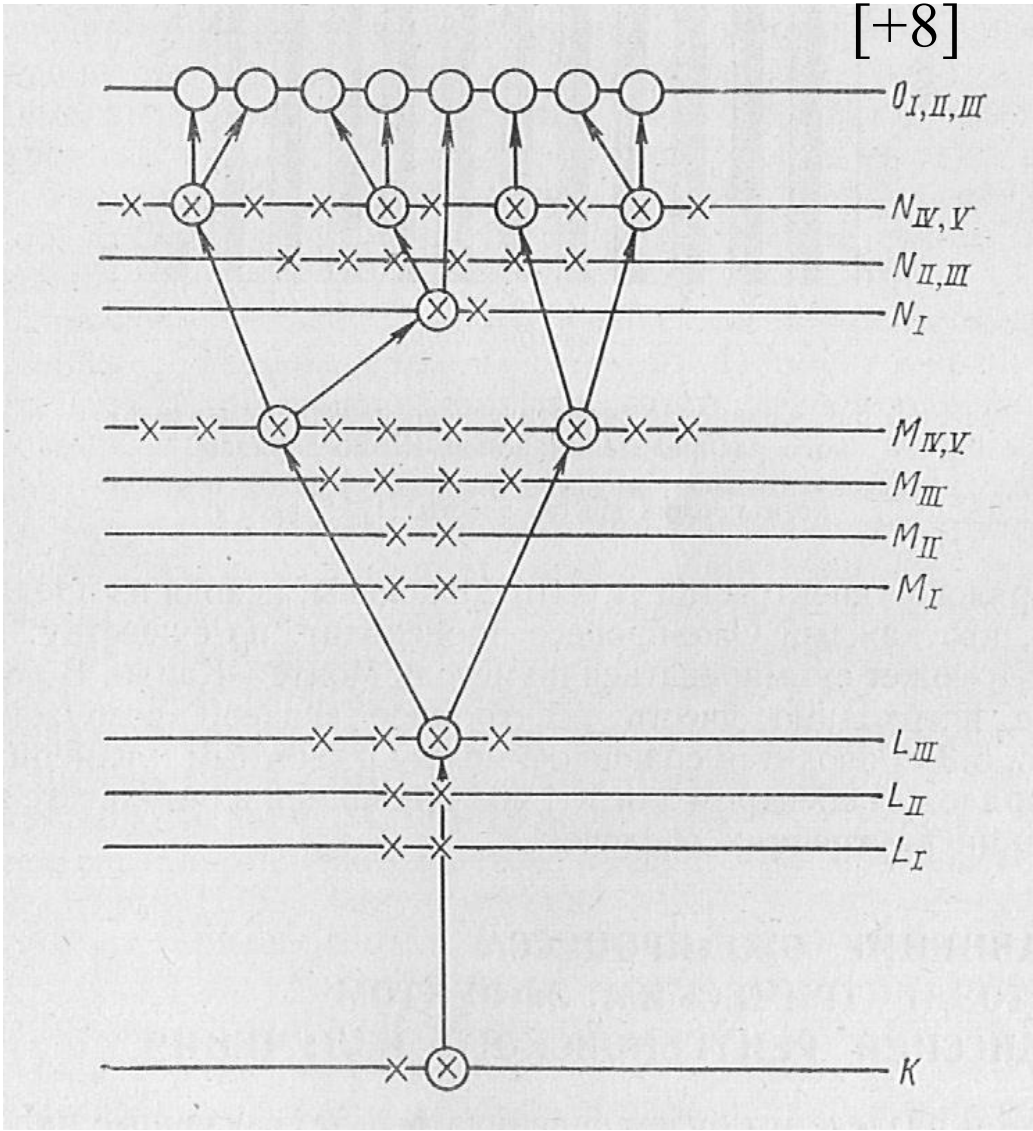

Homework

a) A Xe atom is excited by **100 eV** electrons. Calculate the possible kinetic energies of the resulting Auger electrons.

b) The excitation energy is then increased to **200 eV**. What additional Auger electron energies can be observed?

Xe ground state electron configuration:

$$\mathrm{Xe} : 1s^2\,2s^2\,2p^6\,3s^2\,3p^6\,4s^2\,3d^{10}\,4p^6\,5s^2\,4d^{10}\,5p^6$$

Electron shell		Binding energy (eV)
O III	$5p_{3/2}$	12
O II	$5p_{1/2}$	13
O I	5s	23
N VI	$4f_{5/2}$	-
N VII	$4f_{7/2}$	-
N V	$4d_{5/2}$	68
N IV	$4d_{3/2}$	70
N III	$4p_{3/2}$	146
N II	$4p_{1/2}$	147
N I	4s	213
M V	$3d_{5/2}$	676
M IV	$3d_{3/2}$	689
M III	$3p_{3/2}$	941
M II	$3p_{1/2}$	1002
M I	3s	1149
L III	$2p_{3/2}$	4786
L II	$2p_{1/2}$	5107
L I	2s	5453
K	1s	34561

Auger-Meitner transition probabilities

- Auger-Meitner decay is not strongly restricted by selection rules. Any energetically allowed combination of shells can contribute on the condition:
  $E_{AM}=E_i-E_1-E_2>0$

- Coster-Kronig transitions, where the initial and final vacancies belong to subshells of the same principal shell, are particularly probable because of large wavefunction overlap.

  Example: L_1L_2M (2s2p3d, 2s2p3p)

- Since many decay pathways are possible, Auger cascades can be modeled using Monte Carlo simulations. Reliable simulations require accurate probabilities for every radiative and non-radiative transition.

Electron and photon spectra emitted during the cascade decay of single vacancy in the K shell (BE 33.2 keV) of the atomic iodine

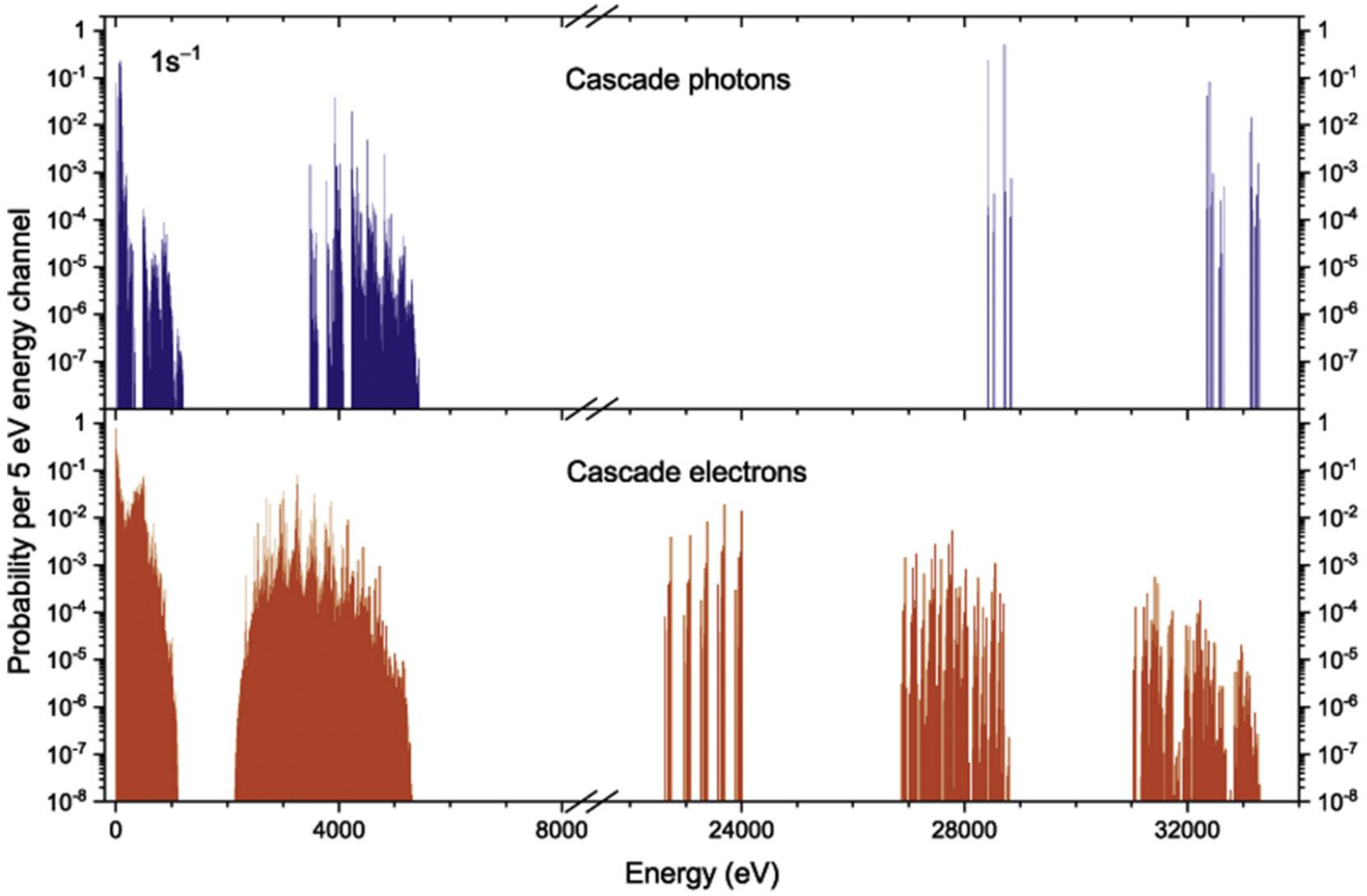

Cascade calculations:

- Method of construction and analysis of the decay trees (CADT)
- Monte Carlo approach (randomly chosen sequences)

Chaynikov, A. P.; Kochur, A. G.; Dudenko, A. I. *Journal of Quantitative Spectroscopy and Radiative Transfer* **2024**, *322*, 109024.

Electron and photon spectra emitted during the cascade decay of single vacancy in the L shell of the atomic iodine

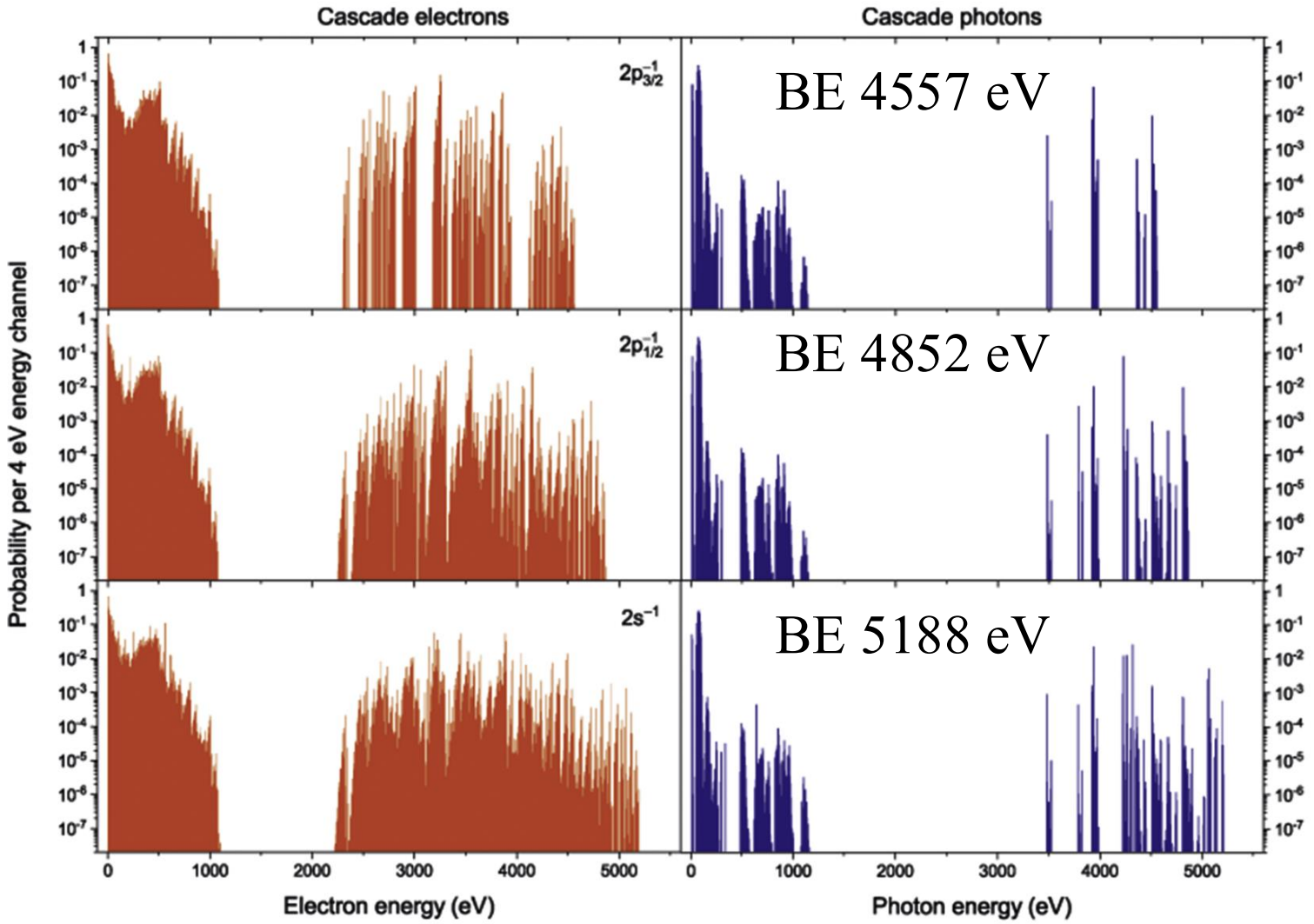

Chaynikov, A. P.; Kochur, A. G.; Dudenko, A. I. *Journal of Quantitative Spectroscopy and Radiative Transfer* **2024**, *322*, 109024.

APPLICATIONS

AES instrumentation

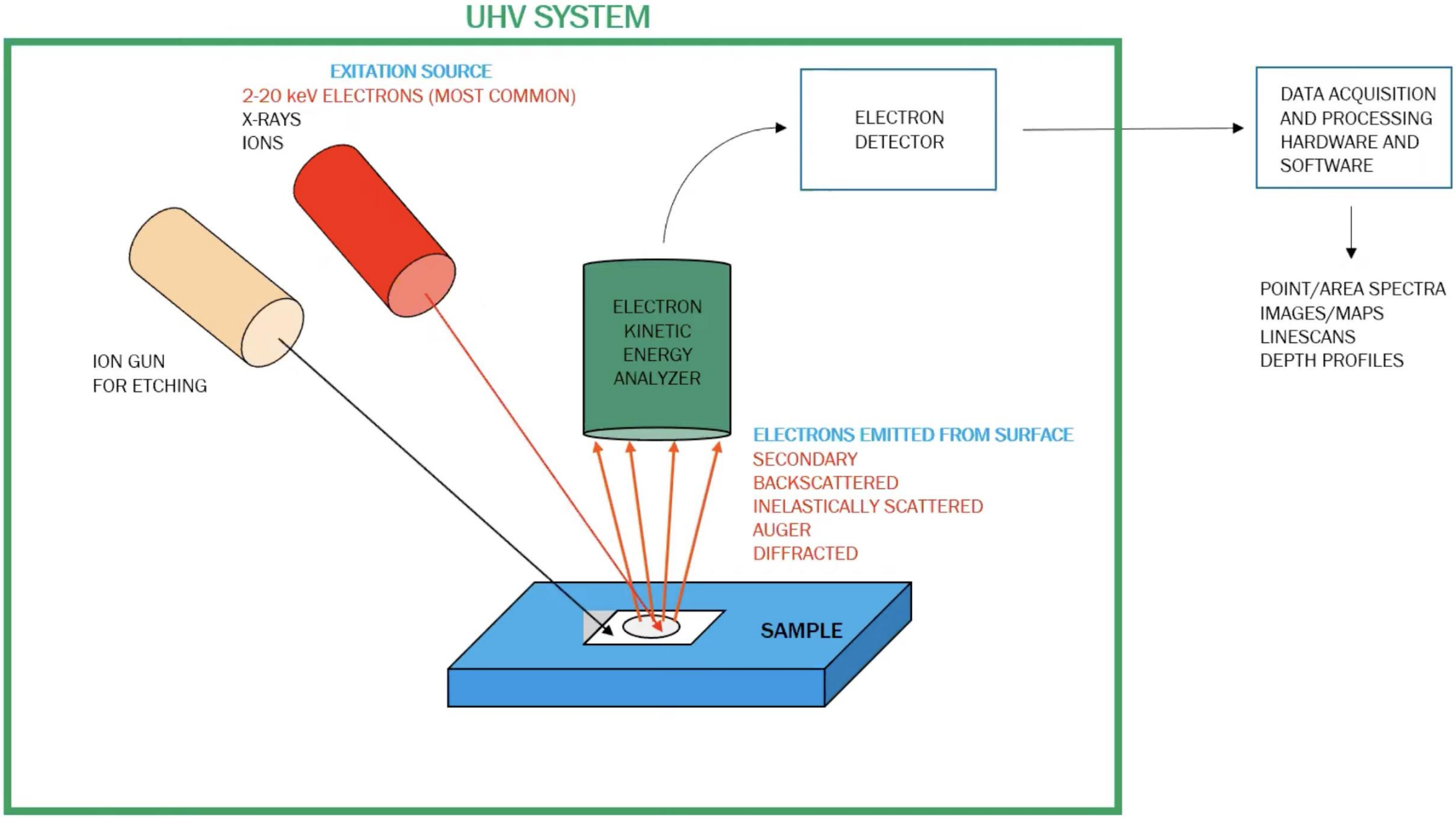

https://www.youtube.com/watch?v=Mw7y4DeddCA

Typical Analysis Depths for Techniques

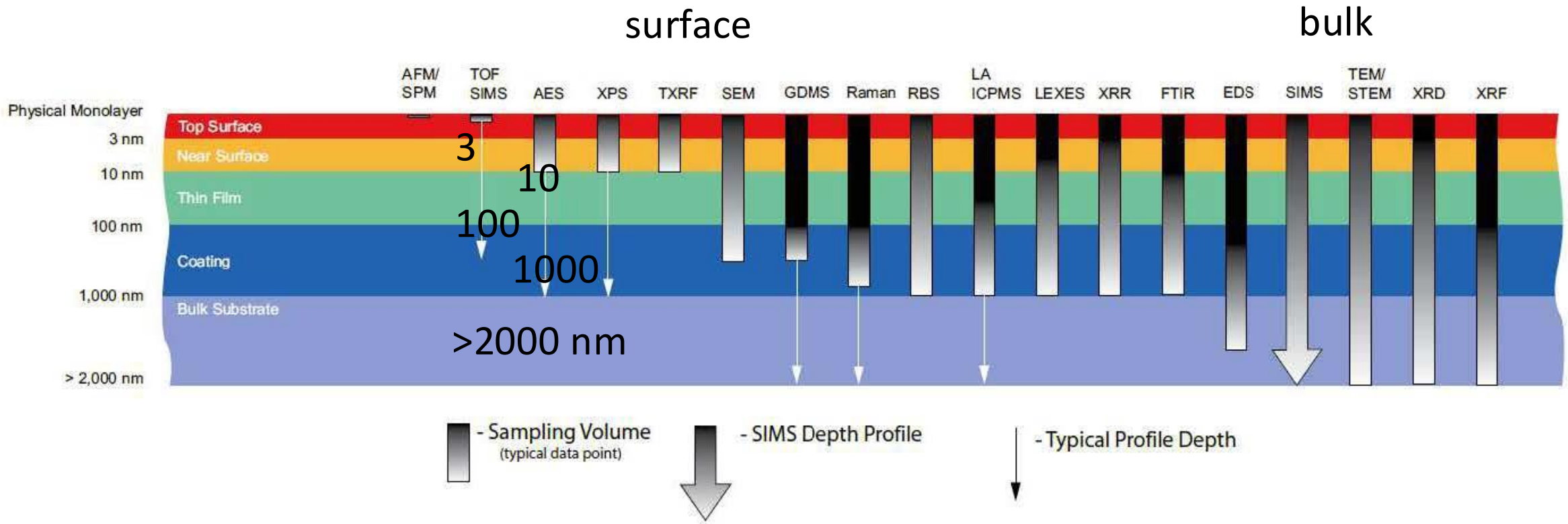

Modes of data acquisition

Point or area mode (spectra)

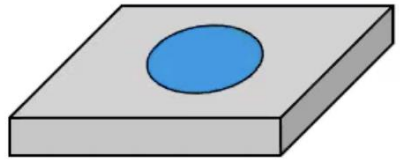

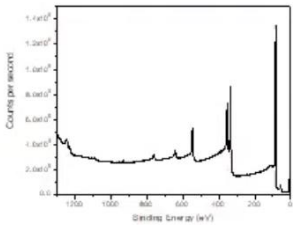

Line scan (1-D surface scan)

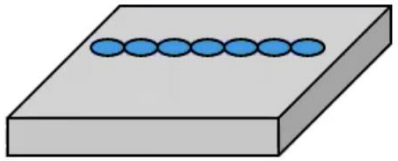

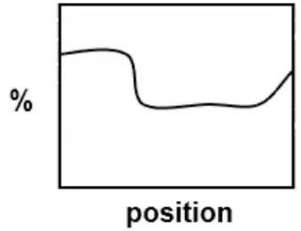

Depth Profile (multiple areas within the etch crater)

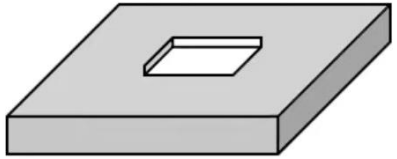

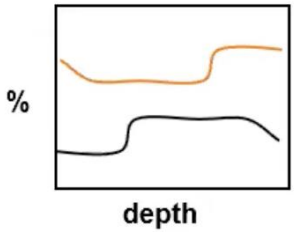

Imaging (2-D surface image)

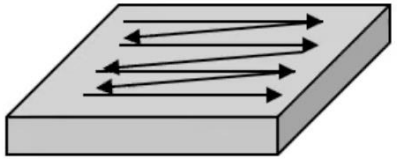

SLIDE COURTESY OF
JEFF SHALLENBERGER

Typical spectra

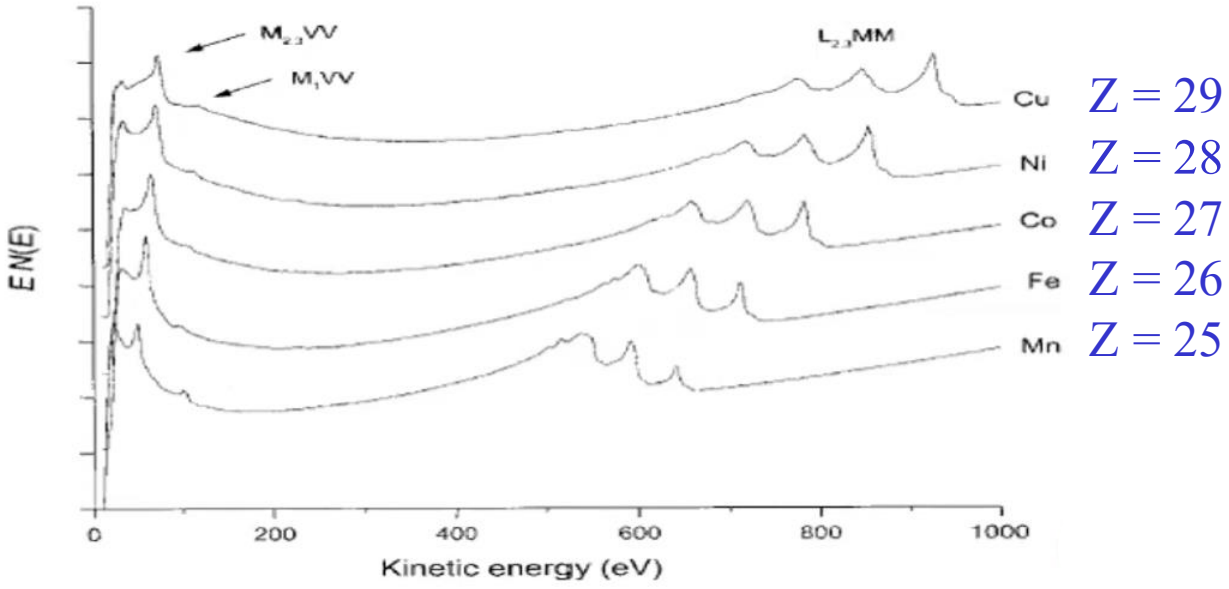

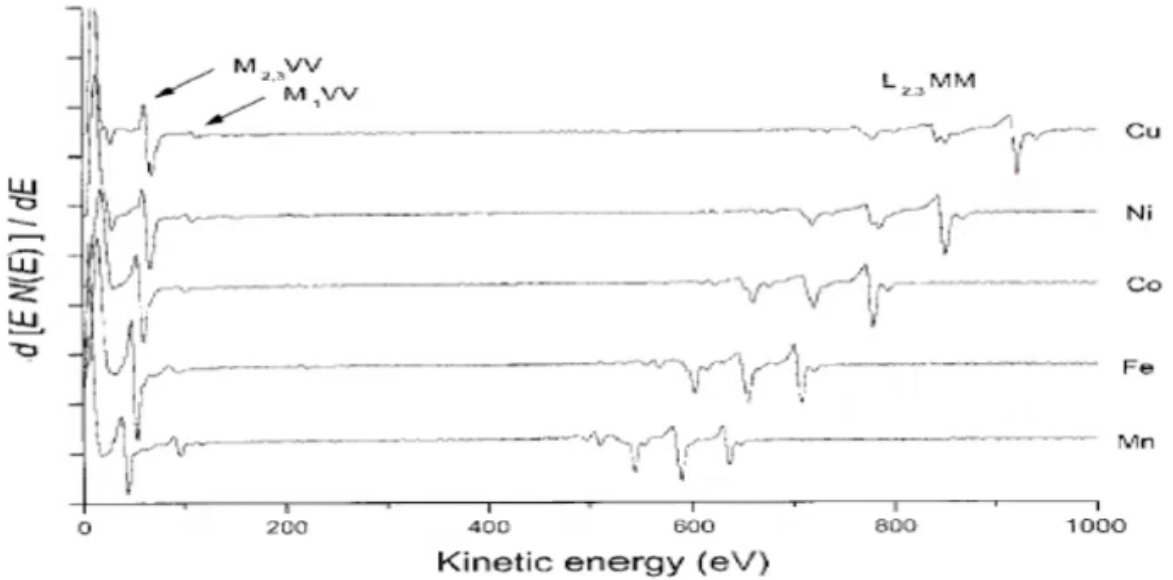

Briggs and Grant, Surface analysis, p. 69

Scanning Auger Microscopy (SAM)

JAMP-9500F – with innovative in-lens Field Emission gun assembly a scanning Auger electron microscope (JEOL, Japan).

Parameters:

- 3 nm lateral resolution in secondary electron image regime;
- **8 nm e-beam diameter** in Auger-analysis, **10 nm lateral resolution** in AES/ESCA regime;
- e-probe current up to 0.5 μA:
- variable energy resolution: 0.05% – 0.6%;
- neutralizing gun for insulator analysis;
- analysis of large samples: support table for samples with diameter up to 95 mm;
- UHV (≤ $5 \cdot 10^{-8}$ Pa (can be ordered: ≤ 1.3×10^{-8} Pa));
- EDS, XPS, SIMS can be added.

Scanning Auger microscopy

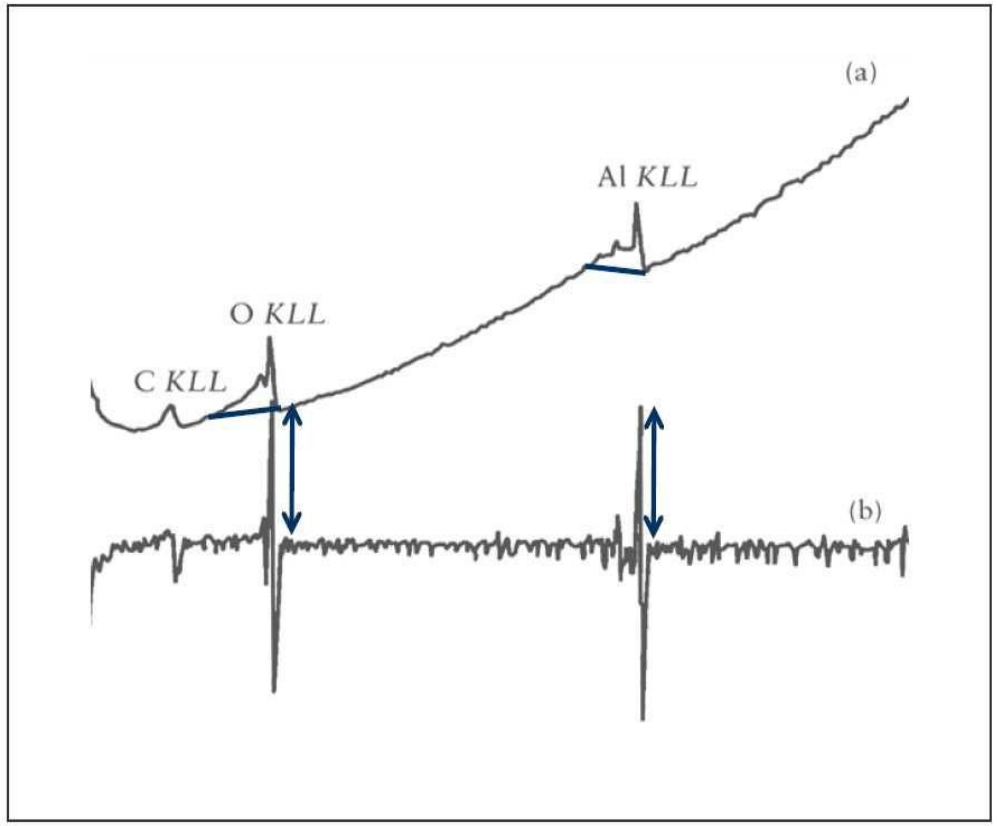

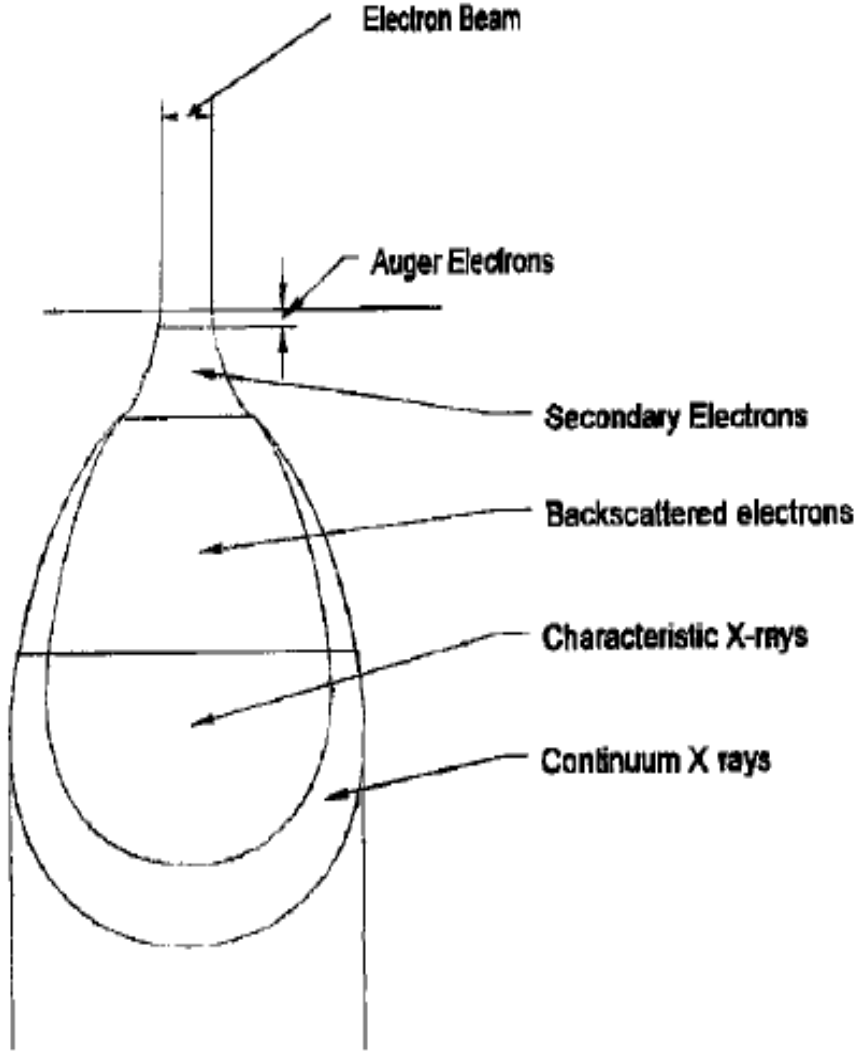

Al_2O_3

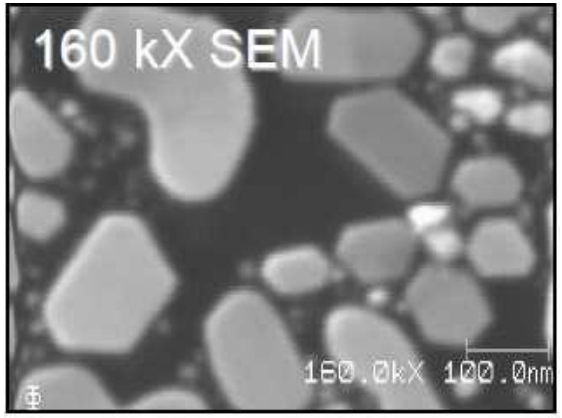

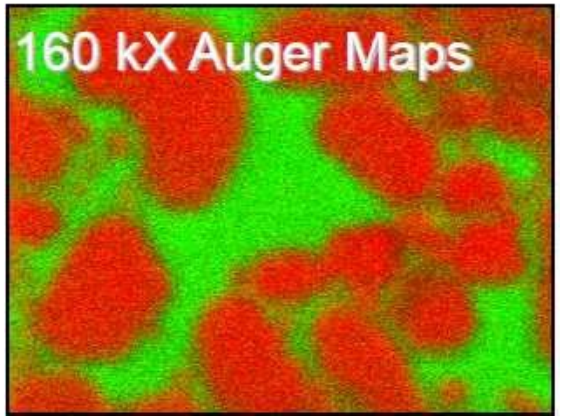

Al is red

source: http://www.uio.no/studier/emner/matnat/fys/MENA3100/v13/undervisningsmateriale/aes_spyros.pdf

Scanning Auger Microscopy (SAM)

Carburised alloy Nicrofer 6025HT

SEM

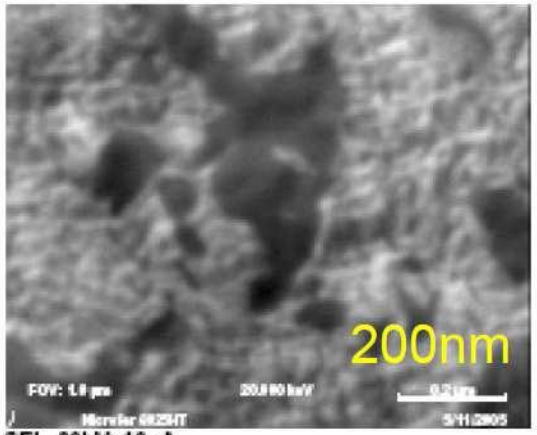

SEI 20kV; 10nA

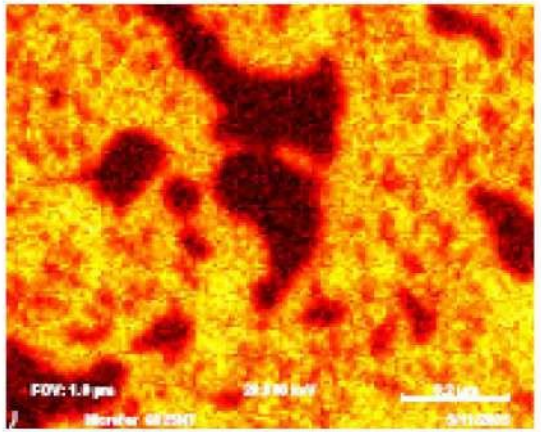
AES Ni Map 20kV; 10nA 128x128 pixels

Ni

Cr

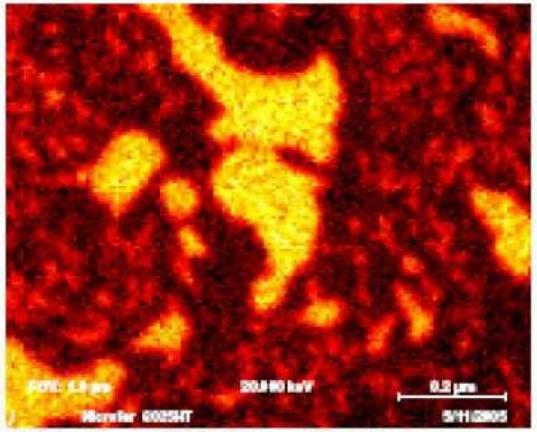
AES Cr Map 20kV; 10nA 128x128 pixels

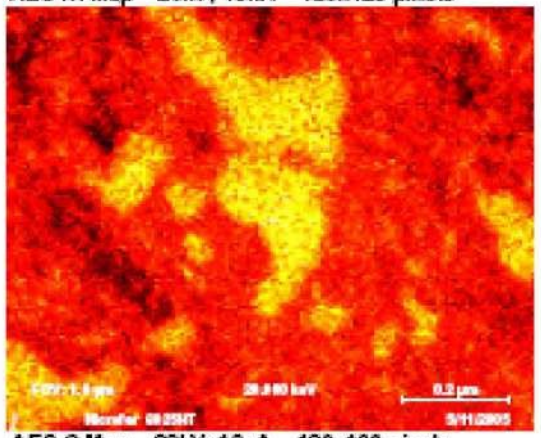
AES C Map 20kV; 10nA 128x128 pixels

C

Yellow regions correspond to the Auger-Meitner electrons coming from a certain element

Elemental mapping of an alloy surface

Image obtained using secondary electrons

Image recorded using tin Auger-Meitner electrons

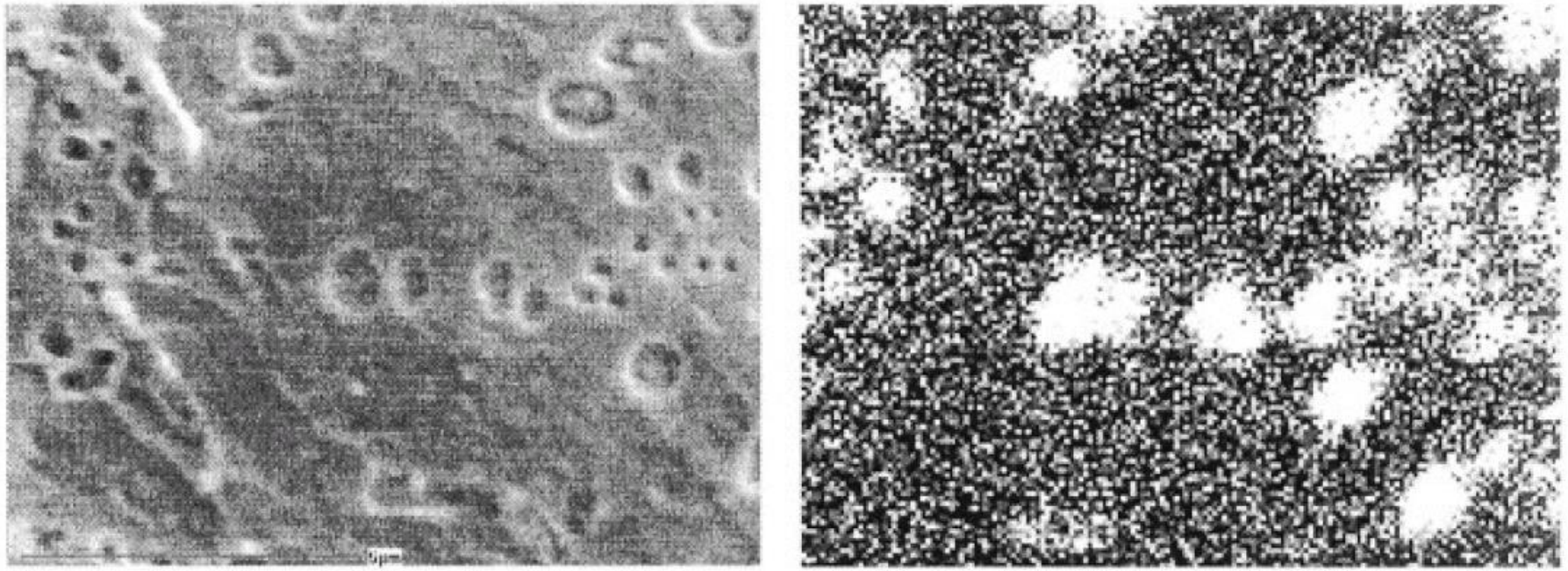

(a) (b)

Figure 6.122. Secondary electron image of a grain boundary in an Fe–3wt%Ni alloy heat treated to produce grain boundary segregation and containing cavities (b) tin Auger element map from region (a) showing tin segregation to cavities (Wild (1977)).

- Spatial resolution: 100 nm

Depth profiling

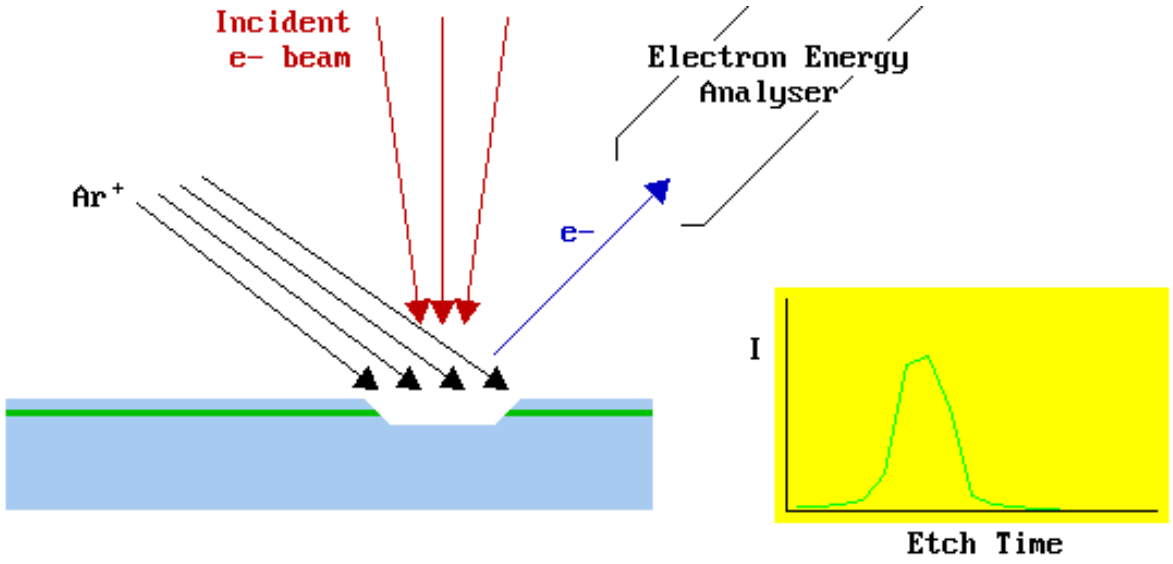

CeO_2 on top of Si substrate

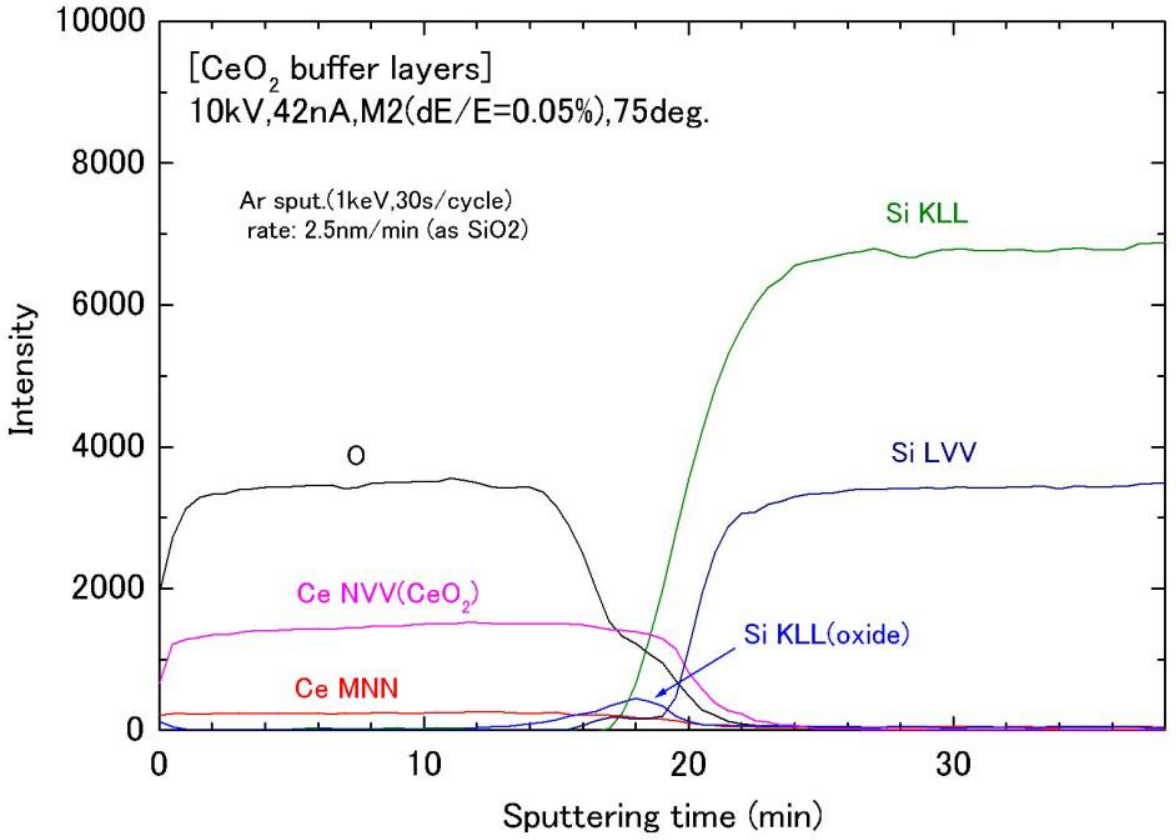

Auger-Meitner electrons in cancer therapy (use of cascades)

- There are two ways to obtain cascade-decaying heavy atoms with inner-shell vacancies within a tumor.
  - Introduction of **unstable isotopes of high-Z elements**. ^{125}I isotopes are often used for this purpose. Vacancies are created by nuclear processes.
  - Introduction of **stable high-Z radiosensitizer isotope**s (e.g., ^{127}I). Photon activation therapy (PAT). Vacancies are created by X-ray irradiation.

Cascade-produced electrons can cause single or double strand breaks in the DNA of cancer cells either by direct inelastic interaction with the DNA molecular groups, or indirectly, by forming aggressive reactive oxygen species through interaction with water molecules.

A clinically exploited effect – with molecular mechanisms unknown

Ongoing clinical trial:
Auger Molecular Therapy (AMT) for Malignant Cutaneous Lesions Treatment
https://www.trialx.com/clinical-trials/listings/305754/auger-molecular-therapy-amt-for-malignant-cutaneous-lesions-treatment/

NanoRay Biotech source:
Autron Therapy System

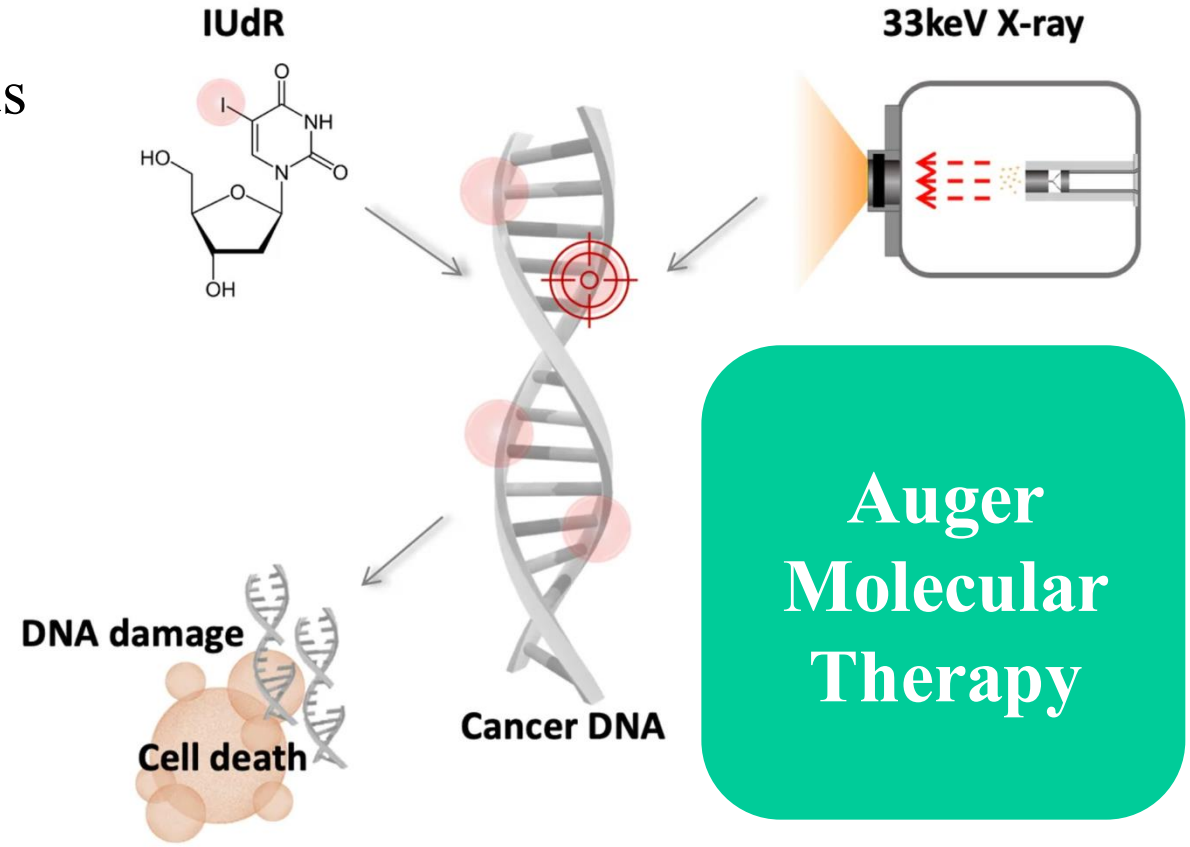

https://nanoray.com/e/

Treated as a black box:
photon absorbed, Auger cascade, DNA damage, cell die

DNA replication with halogenated radiosensitizer

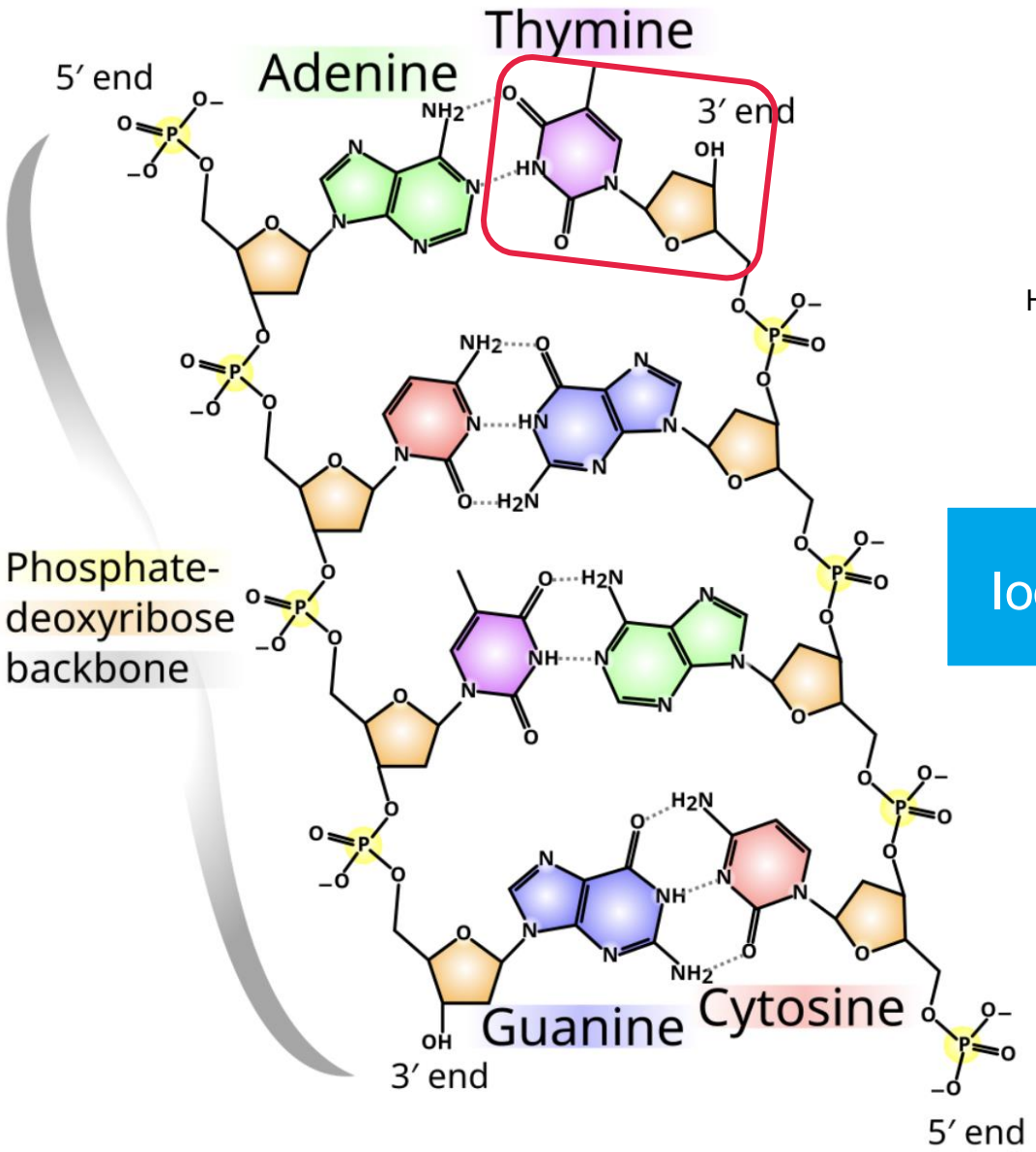

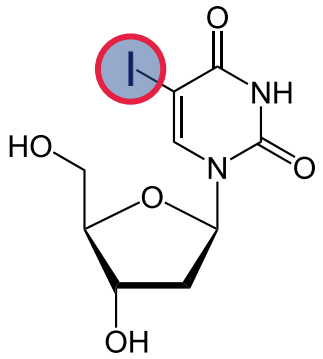

Iododeoxyuridine, IUdR

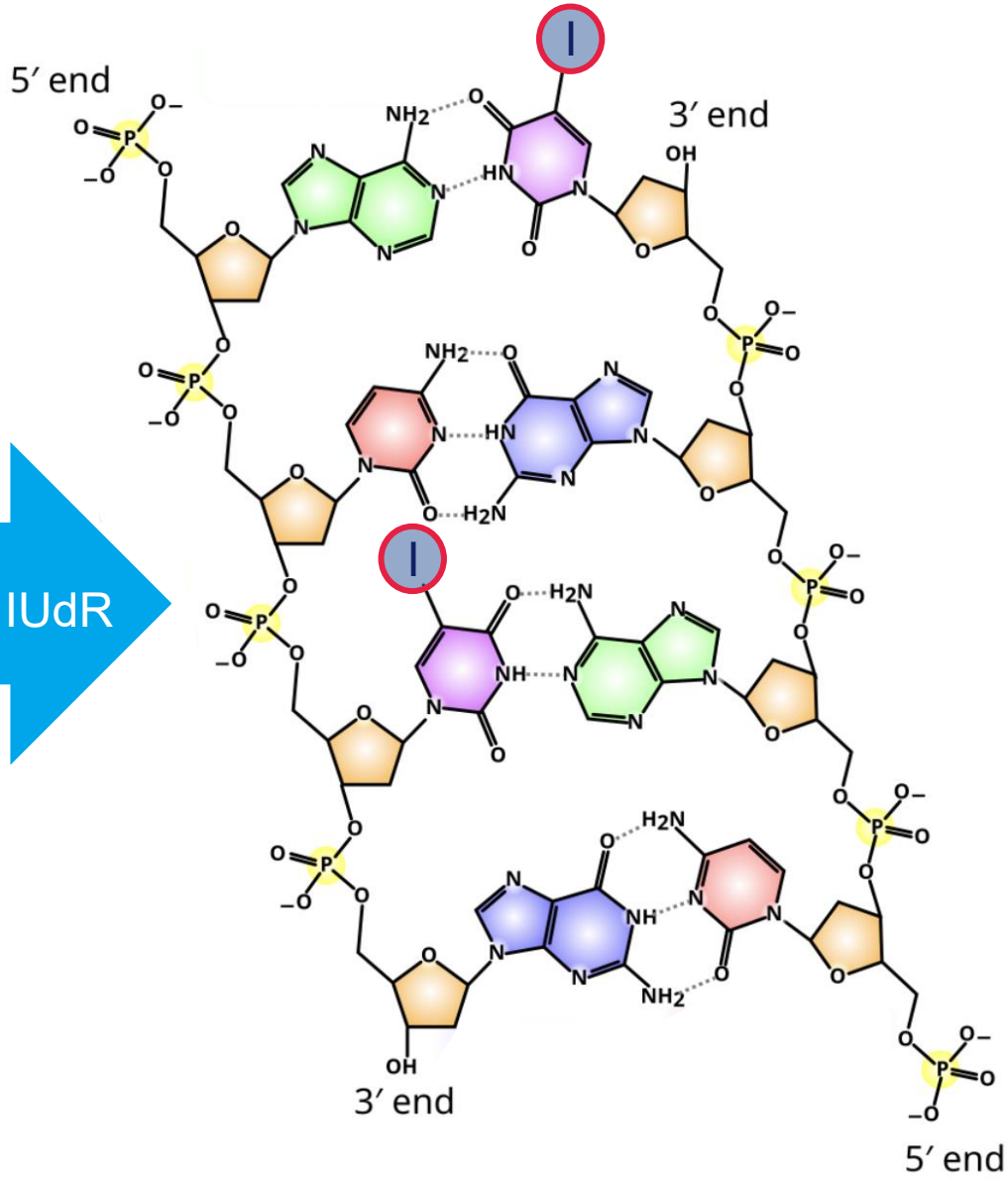

DNA structure done by Madeleine Price Ball

High-Z atom as an X-ray antenna

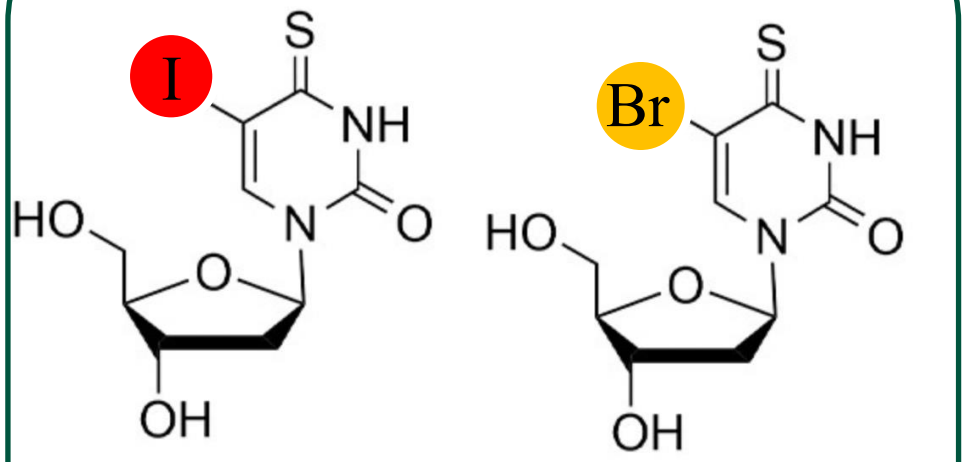

Deoxyuridines

Pusa, K.-I, M.; Travnikova, O. *Phys. Chem. Chem. Phys.* **2026**, *28* (16), 10414–10427.

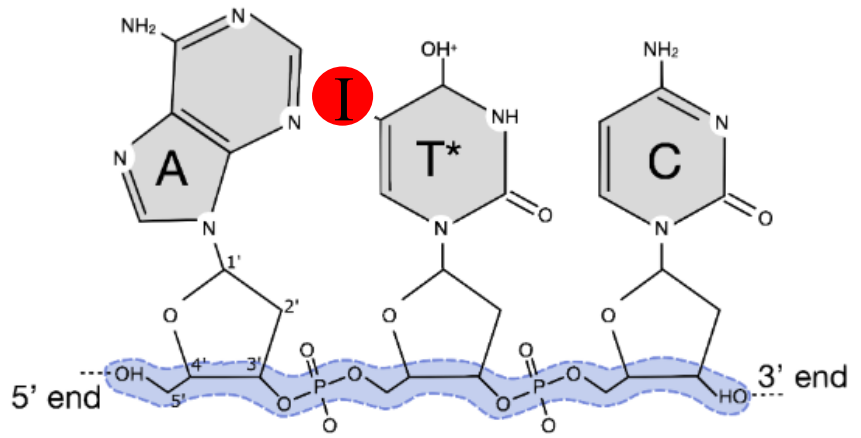

Iodinated DNA oligonucleotides

Svensson, P. H. W., Caleman, C. *Chem. Sci.* **2025**. *16* (41), 19235–19243

Hafiani, O. H.; Svensson, P. H. W. *Phys. Med. Biol.* **2026**, *71* (3), 035010.

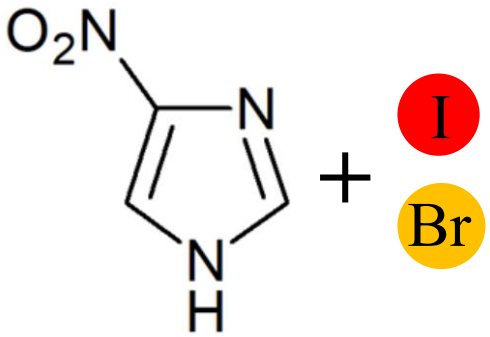

Nitroimidazoles

Pihlava L., Kukk E. et al., PCCP, **2023**, 25, 13004-13011

Pihlava L., Berholts M. et al., PCCP, **2024**, 26, 8879-8890

Svensson, P. H. W.; Berholts, M. *Phys. Chem. Chem. Phys*. **2024**, *26* (2), 770–779.

Photon absorption cross-sections

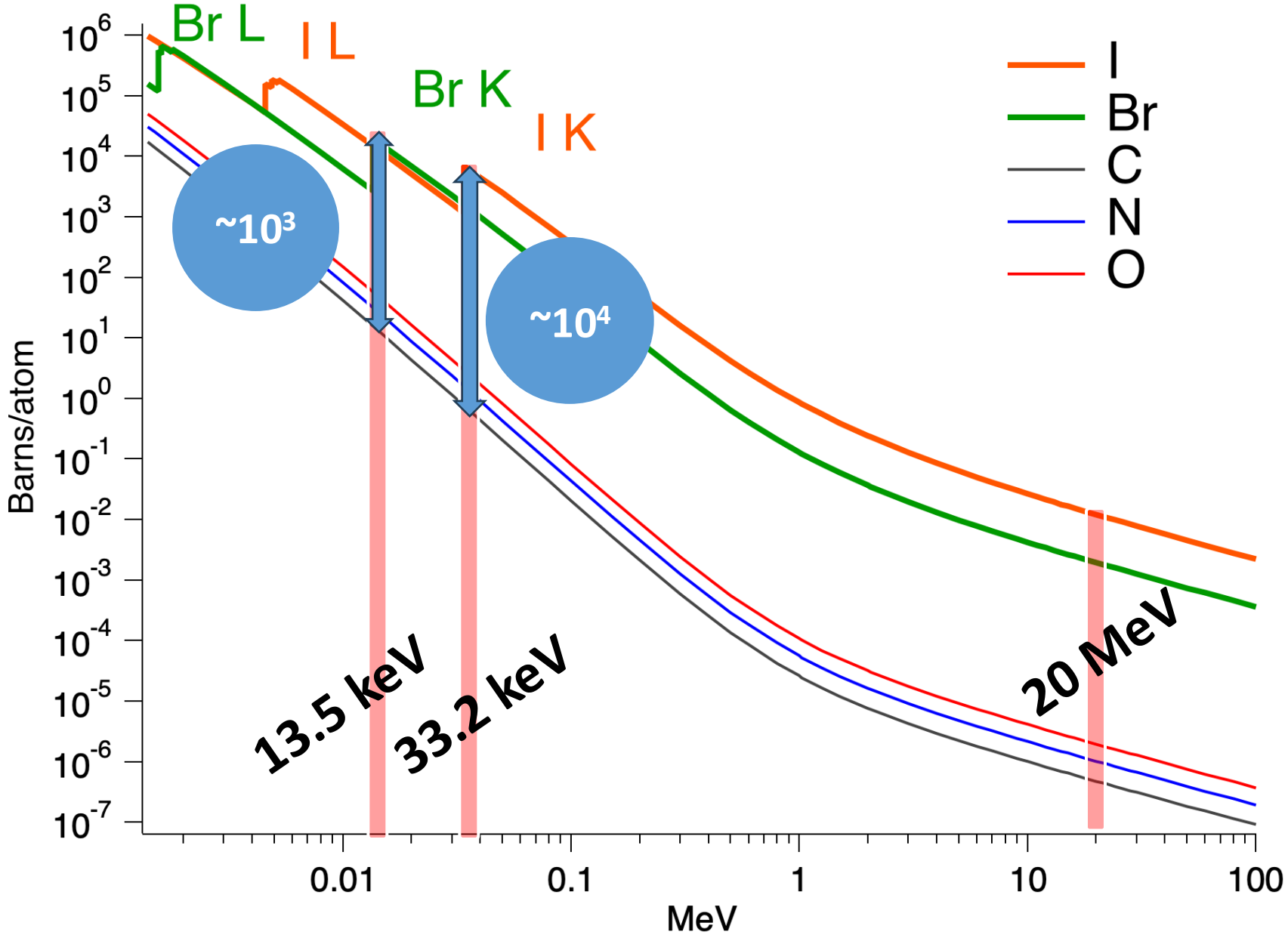

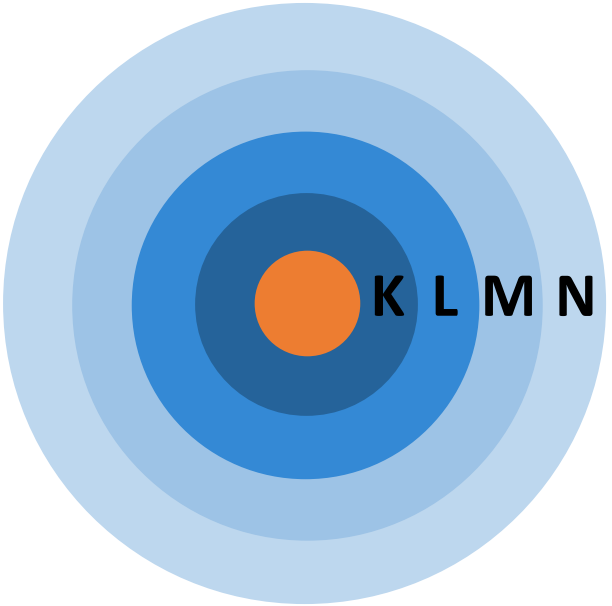

Halogen atom as an X-ray antenna

XCOM: Photon Cross Sections Database

Motivation to improve cancer radiotherapy by understanding radiosensitizers' structure-property relashionship to develop predictive models for their behavior

- **Radiosensitizers (RS)** – radiotherapy enhancers, destroy cancerous cells when exposed to X-rays -> require activation by radiation
- How to make an efficient RS? We need to understand how the RS could be activated in radiotherapy.
- Clinical studies can show which RS is better performing.
- Fundamental molecular level research can look for the clues "why?".

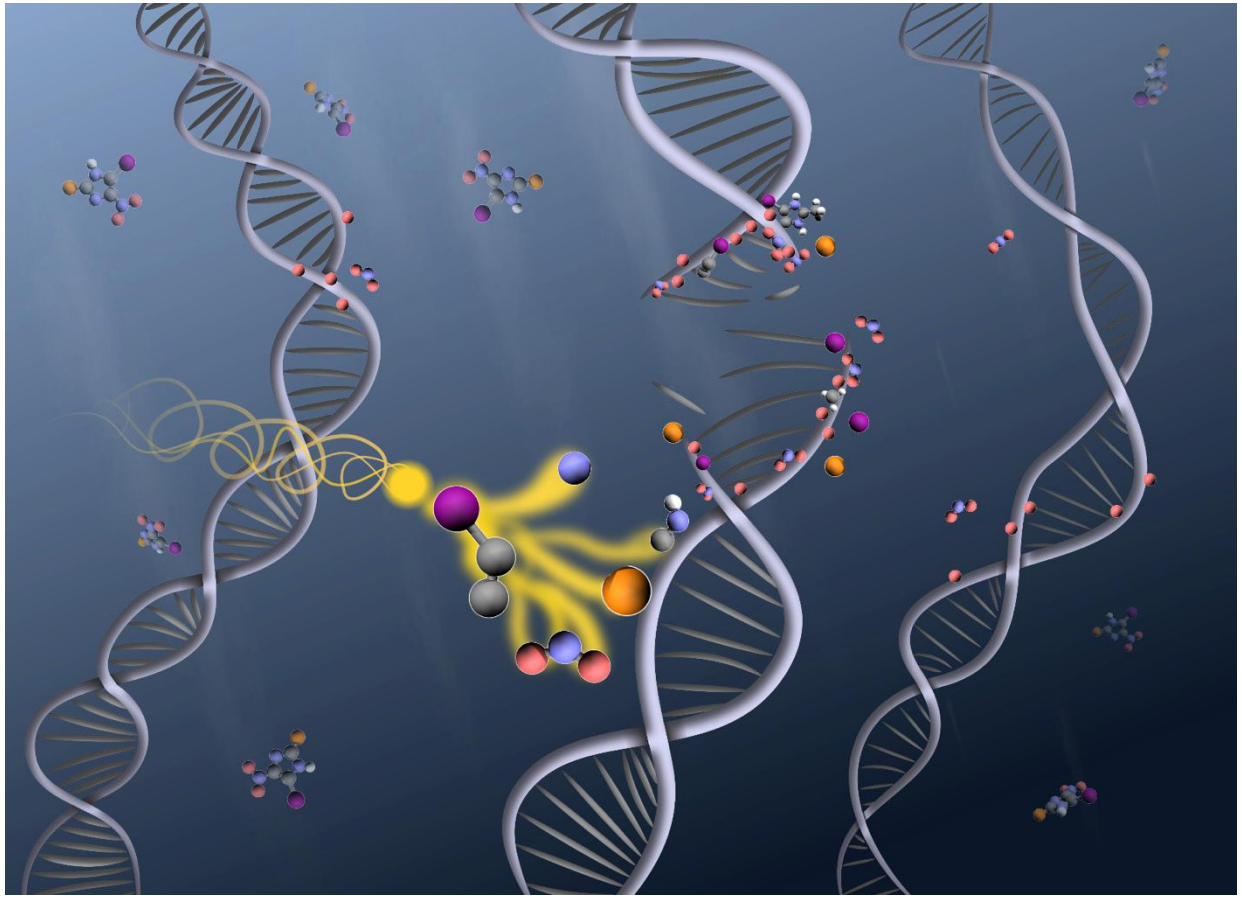

Illustration by Dr. Pamela Svensson

Biological damage caused by high-energy photon radiation (keV to MeV)

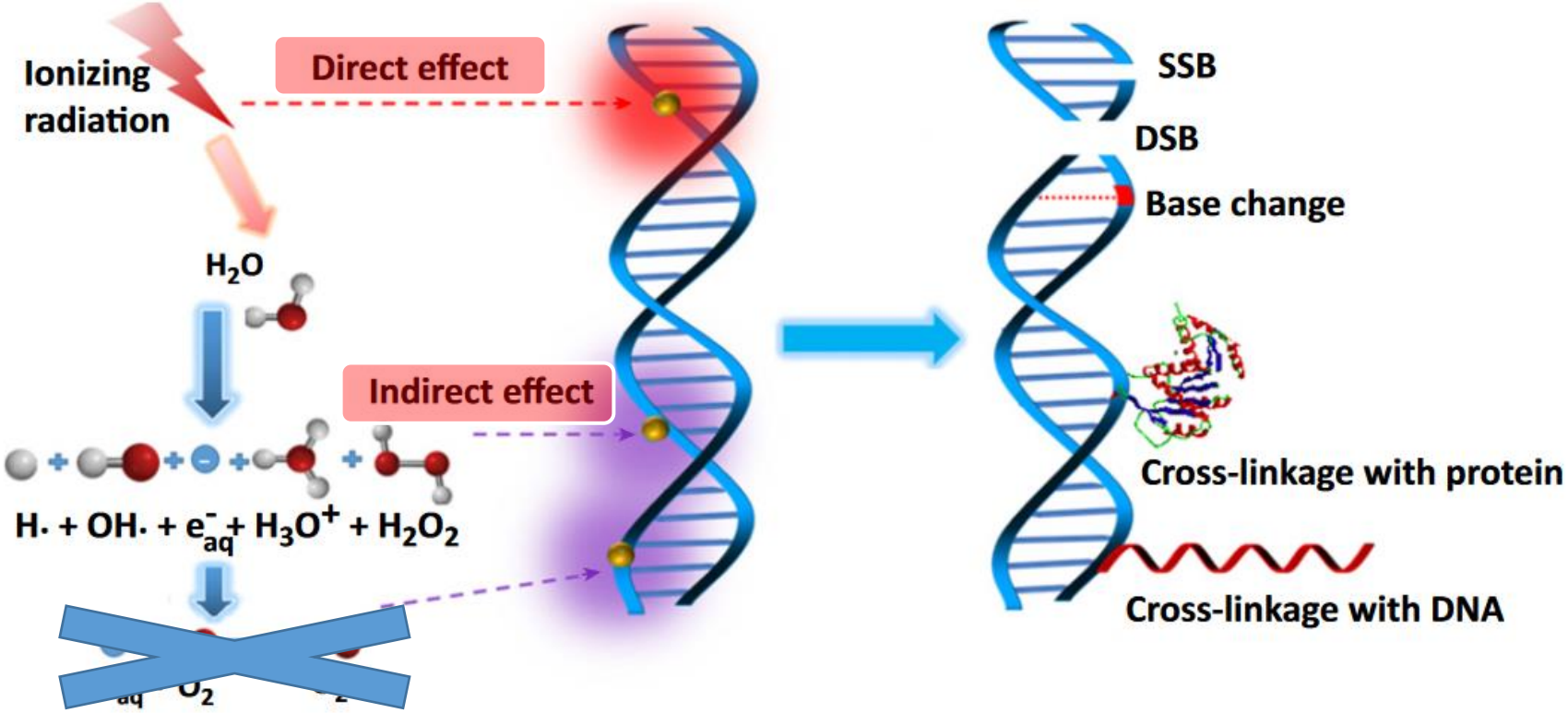

Radiation therapy = radical therapy

Wang H, Mu X, He H, Zhang X-D. Cancer Radiosensitizers. *Trends Pharmacol Sci*. 2018;39(1):24-48.

Tumour hypoxia – common cause of failure in radiotherapy

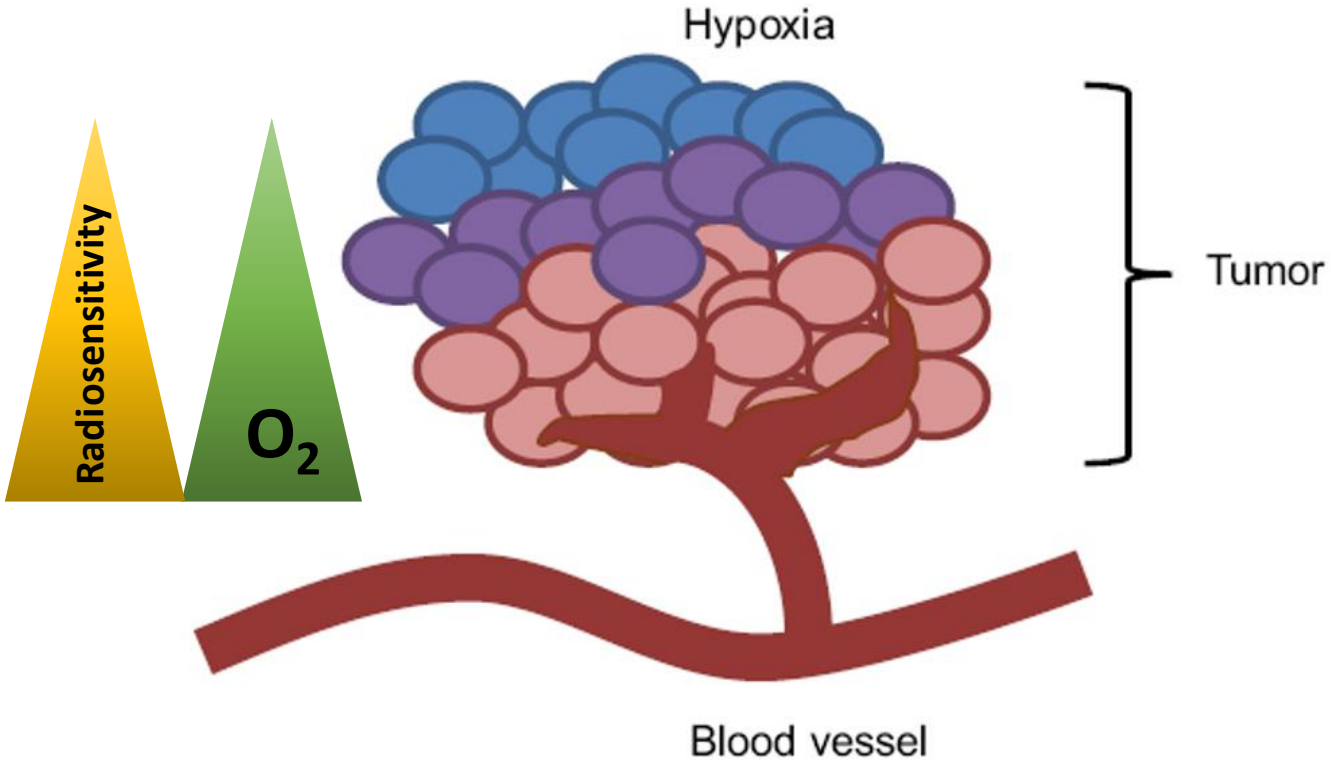

Hypoxic tumours require x3 higher radiation doses!

Graham K, Unger E. Overcoming tumor hypoxia as a barrier to radiotherapy, chemotherapy and immunotherapy in cancer treatment. *Int J Nanomedicine*. 2018;13:6049-6058 https://doi.org/10.2147/IJN.S140462

Biological damage caused by high-energy photon radiation (keV to MeV)

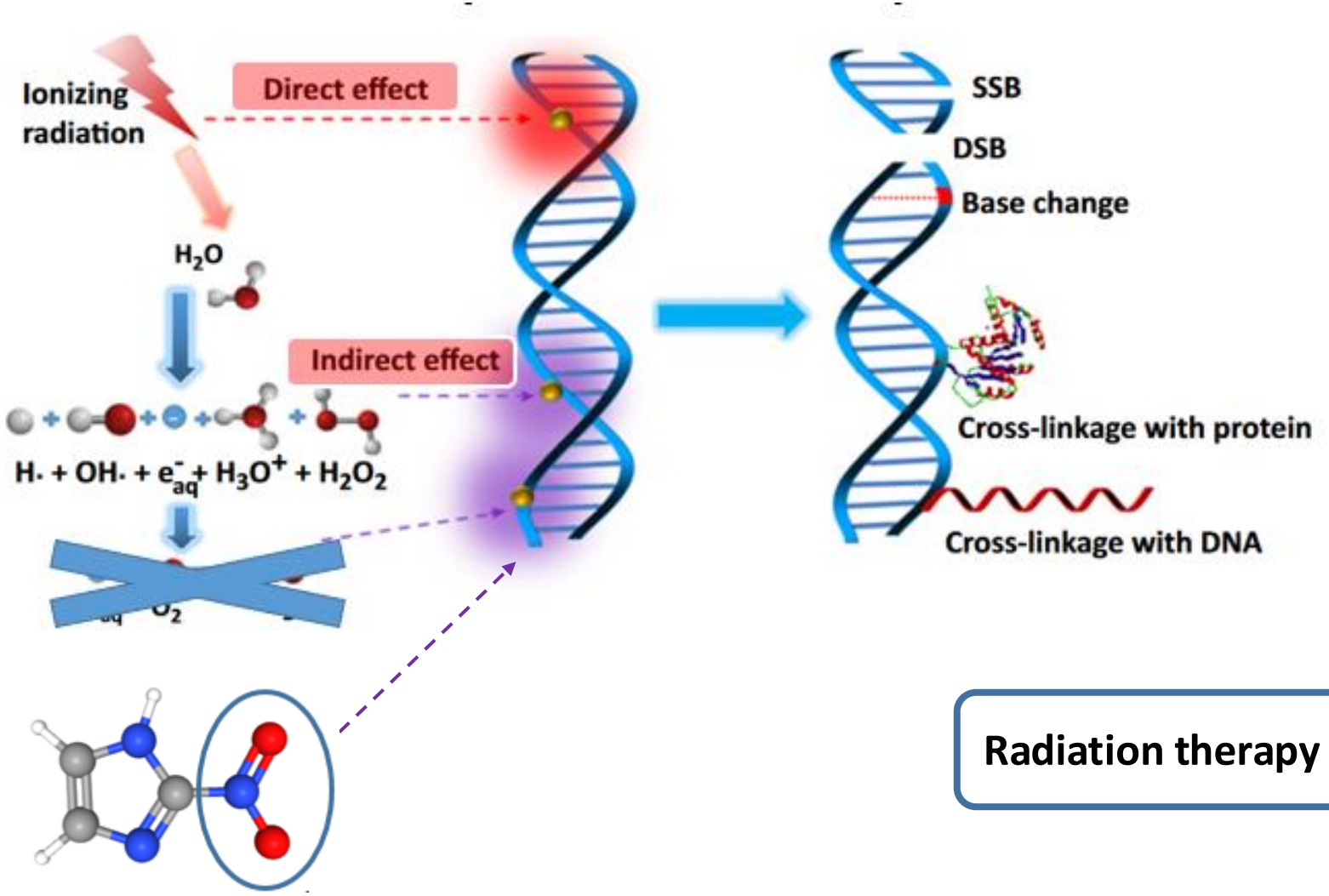

Radiation therapy = radical therapy

Wang H, Mu X, He H, Zhang X-D. Cancer Radiosensitizers. *Trends Pharmacol Sci*. 2018;39(1):24-48.

Examples of nitroimidazole-based radiosensitizers studied in clinical trials

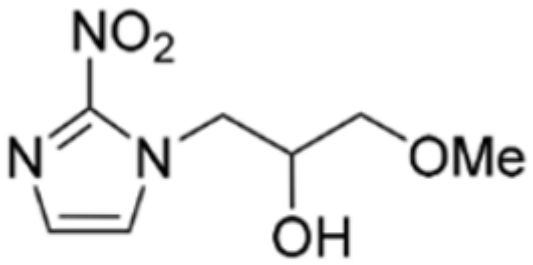

Misonidazole

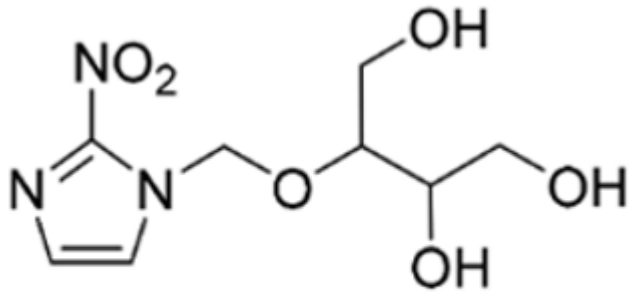

Doranidazole

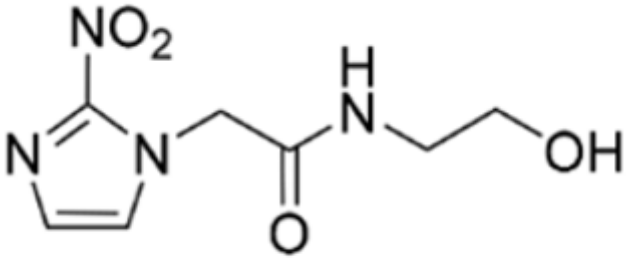

Etanidazole

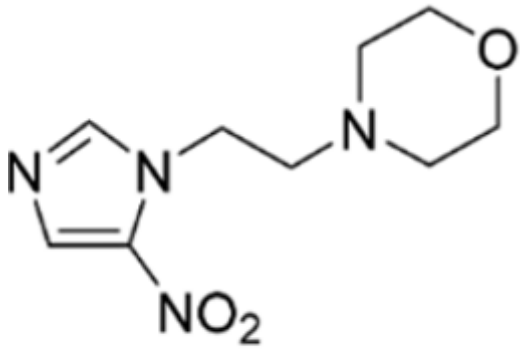

Nimorazole

Combining two sensitization types in one molecule

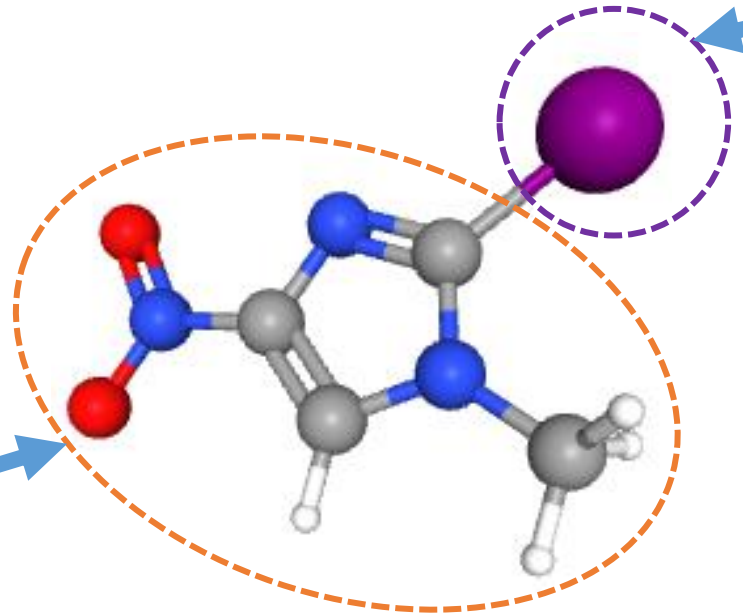

HIGH-Z ELEMENT

- Increased photon and electron ionization cross section -> more localized absorbed dose
- Auger-Meitner cascades -> higher rate of secondary ionizations

NITROIMIDAZOLE

- Ability to accumulate in hypoxic environment
- O_2 mimics: introduces irreparable damage to DNA (NO_2 group radicals)

Halogen atom as an X-ray antenna

In vitro study on human adenocarcinoma cells

ANTICANCER RESEARCH 25: 2145-2152 (2005)

Iodinated Nitroimidazoles as Radiosensitizers

WERNER KRAUSE[1], ANDREAS JORDAN[2], REGINA SCHOLZ[2] and JOSÉ-LUIS MARTIN JIMENEZ[3]

[1]*Schering AG, Berlin;* [2]*Center of Biomedical Nanotechnology (CBN), c/o Department of Radiology, Charité - University Medicine, Berlin, Germany;*
[3]*Department of Pharmacology and Toxicology, Centro Investigacion Justesa Imagen, S.A. (CIJISA), Madrid, Spain*

Abstract. *Four different nitroimidazole derivatives, with up to two iodine atoms on the imidazole ring, were investigated for their radiosensitizing potency under hypoxic conditions, in order to test whether the introduction of iodine atoms increases the radiosensitizing potency of nitroimidazoles. Misonidazole and* for lower photon energies. At 50 kV, the introduction of iodine atoms seemed to improve the radiosensitizing potency. At 20 MV, the results were not as clear. Potentially, this high energy is not as optimal as lower energies for radiosensitizing purposes.

Why do halogenated nitroimidazoles show improved radiosensitivity close to their core-ionization threshold?

How does the addition of a heavy element influence molecular fragmentation and the production of damaging species?

Coincidence setup @ FinEstBeAMS gas phase end station, MAX IV, Sweden

Electron spectrometer

Ion TOF analyzer

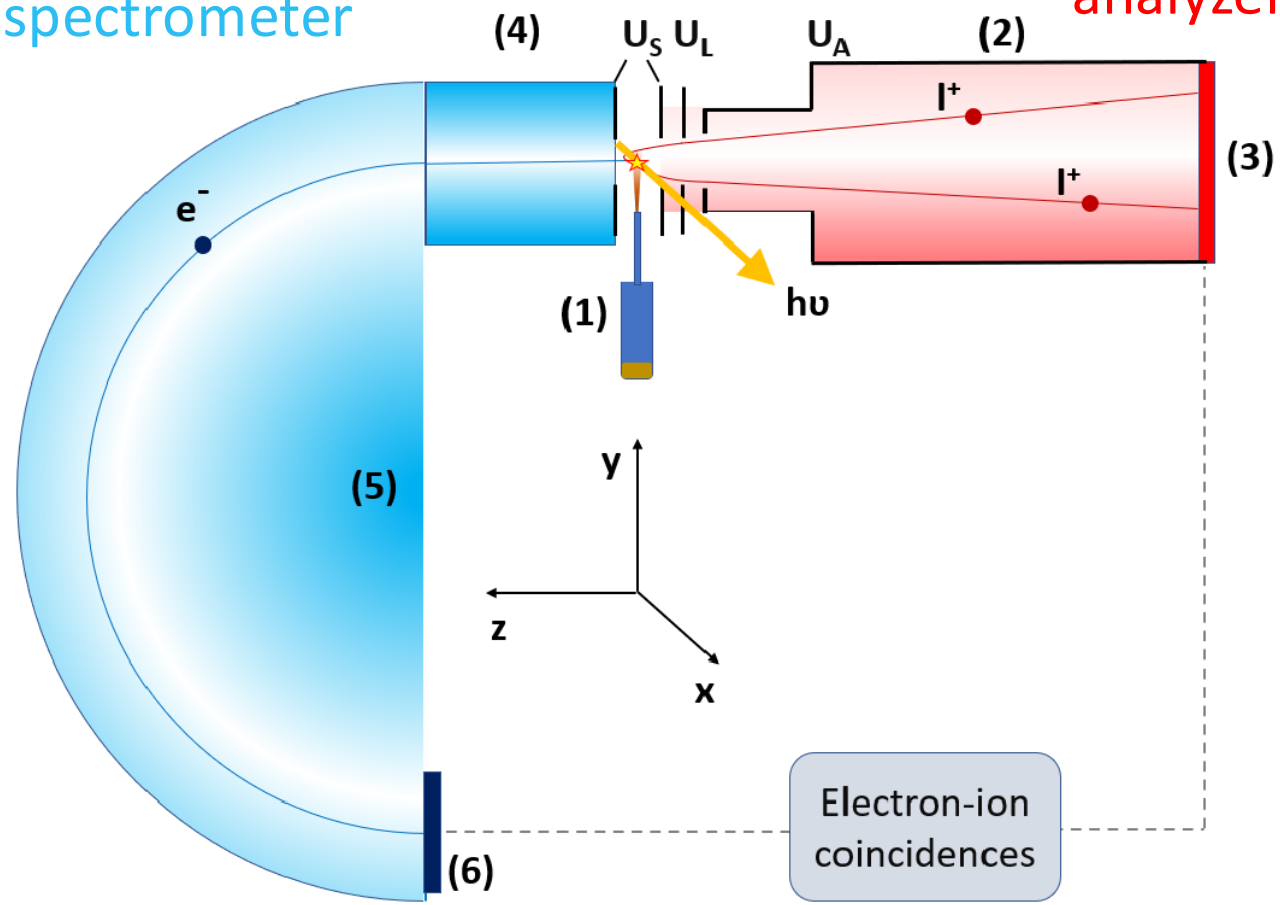

Photoelectron-photoion-photoion coincidence (PEPIPICO)

Event: photoelectron, ion, ion

Pihlava L. et al., Phys. Chem. Chem. Phys., 2021, 23, 21249-21261

Coincidence setup @ FinEstBeAMS gas phase IV, Sweden

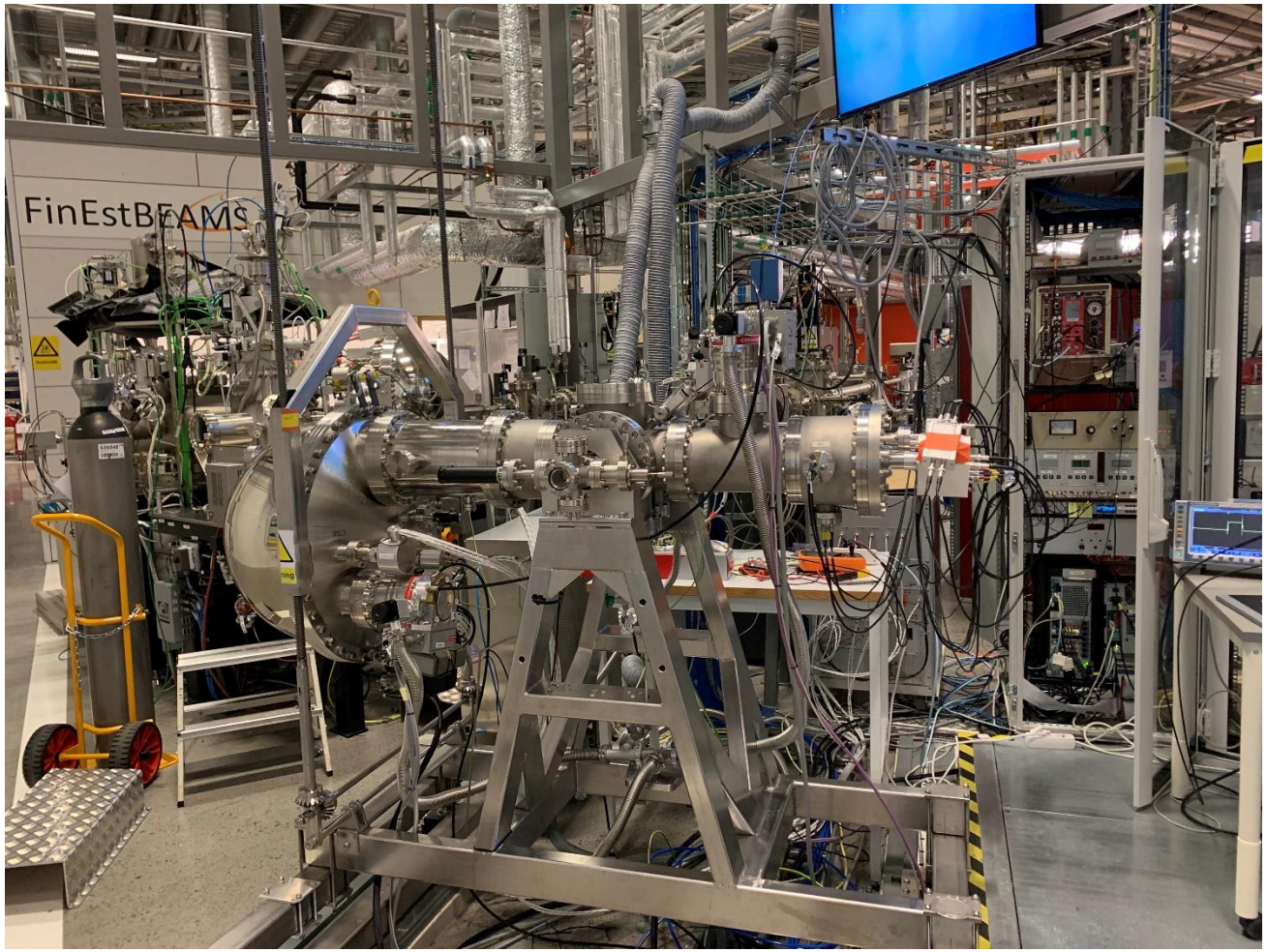

MUSTACHE coincidence setup used at SOLEIL, GALAXIES beamline, Paris

MUlti-STep photofragmentation studies by Auger electron-ion Coincidences using High Energy photons

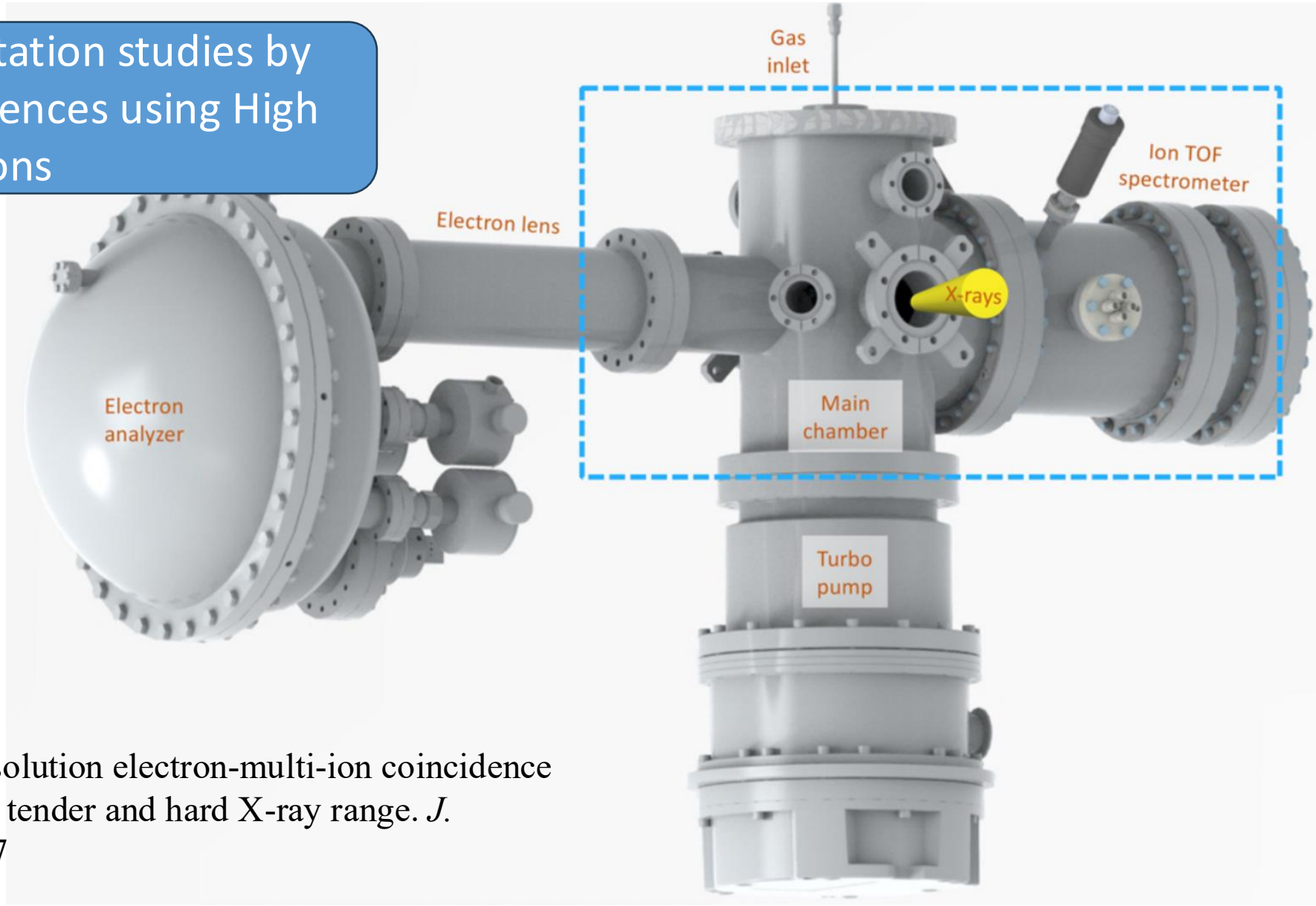

E. Kukk, O. Travnikova et al. High-resolution electron-multi-ion coincidence set-up for gas-phase experiments in the tender and hard X-ray range. *J. Synchrotron Rad. (2025)* 32, 1017-1027

Photofragmentation study №1: brominated nitroimidazoles

Photoion-photoion coincidence map of brominated nitroimidazoles

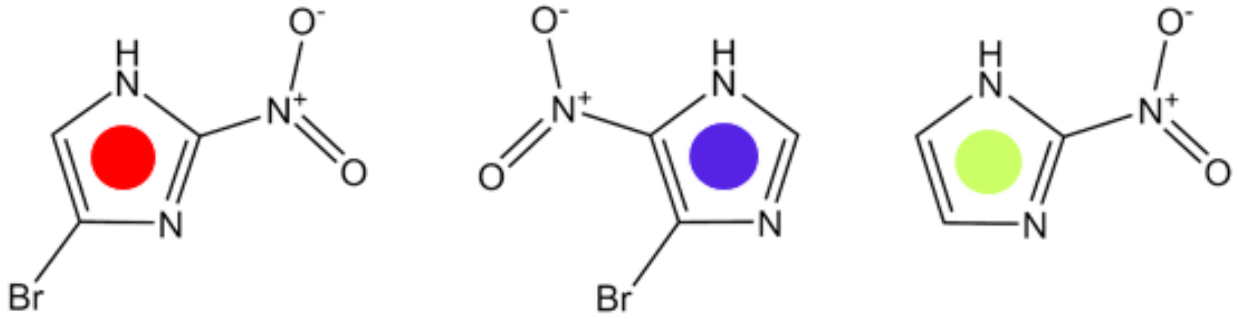

- Enables to study how bromination, the position of the nitro group and the site of the initial ionization influence photofragmentation.

C 1s -> hv = 330 eV
N1s -> hv = 440 eV
Br 3d -> hv = 110 eV
→ Auger-Meitner decay → Dicationic state

- Minor differences between Br 3d vs. C 1s vs. N 1s
- Top coincidences independent on the initial ionization site contain: **NO^+, NO_2^+, O^+, N^+** and **Br^+**

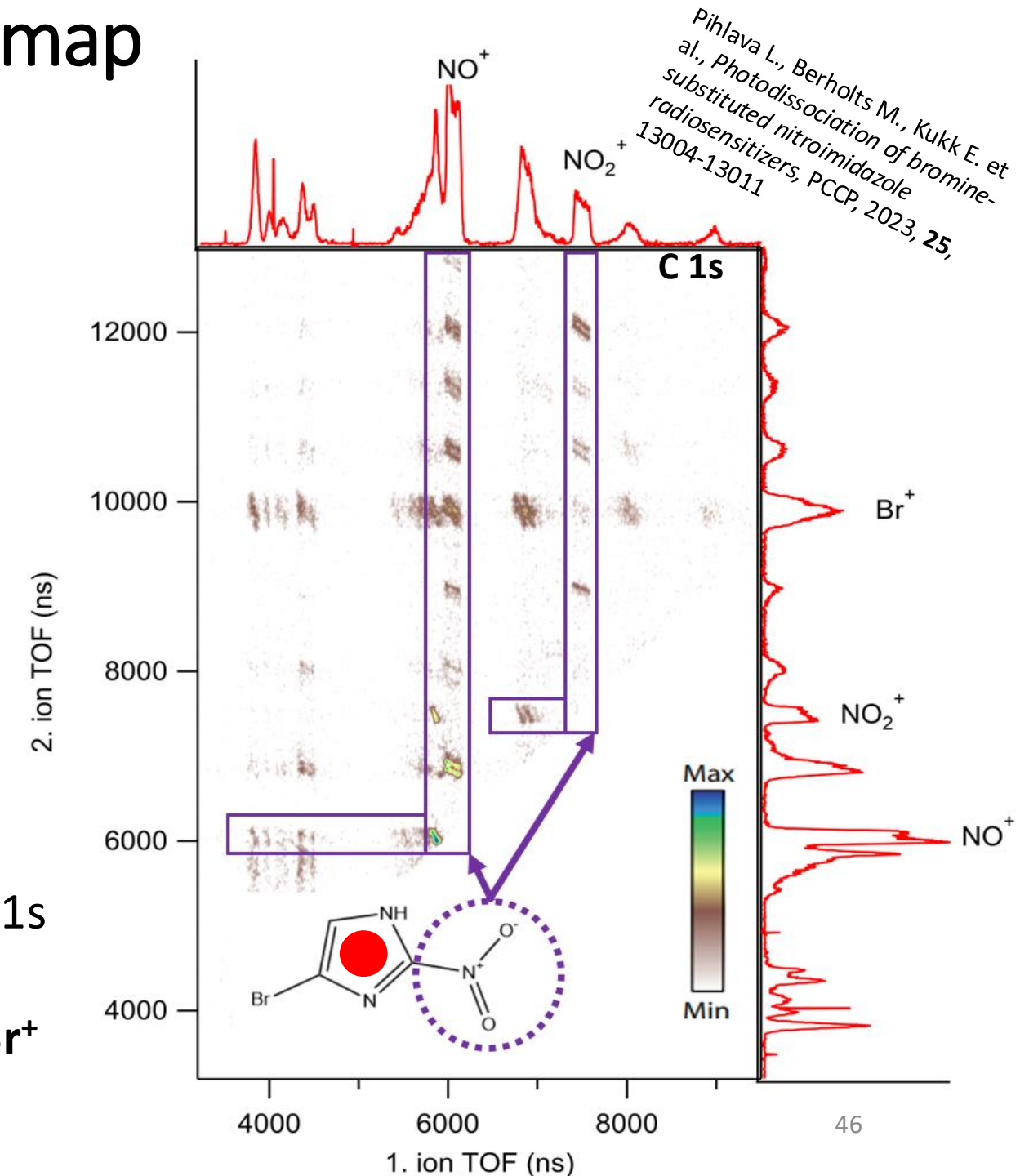

Pihlava L., Berholts M., Kukk E. et al., Photodissociation of bromine-substituted nitroimidazole radiosensitizers, PCCP, 2023, **25**, 13004-13011

MAX IV, FinEstBeAMS

Comparison of the branching ratios between different samples (average across C 1s, N 1s, and Br 3d)

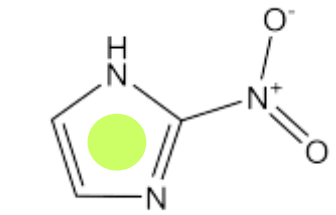

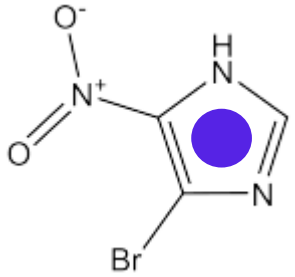

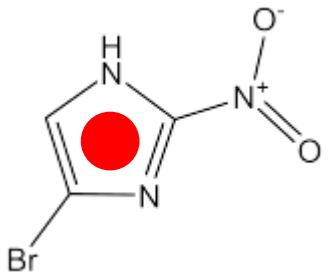

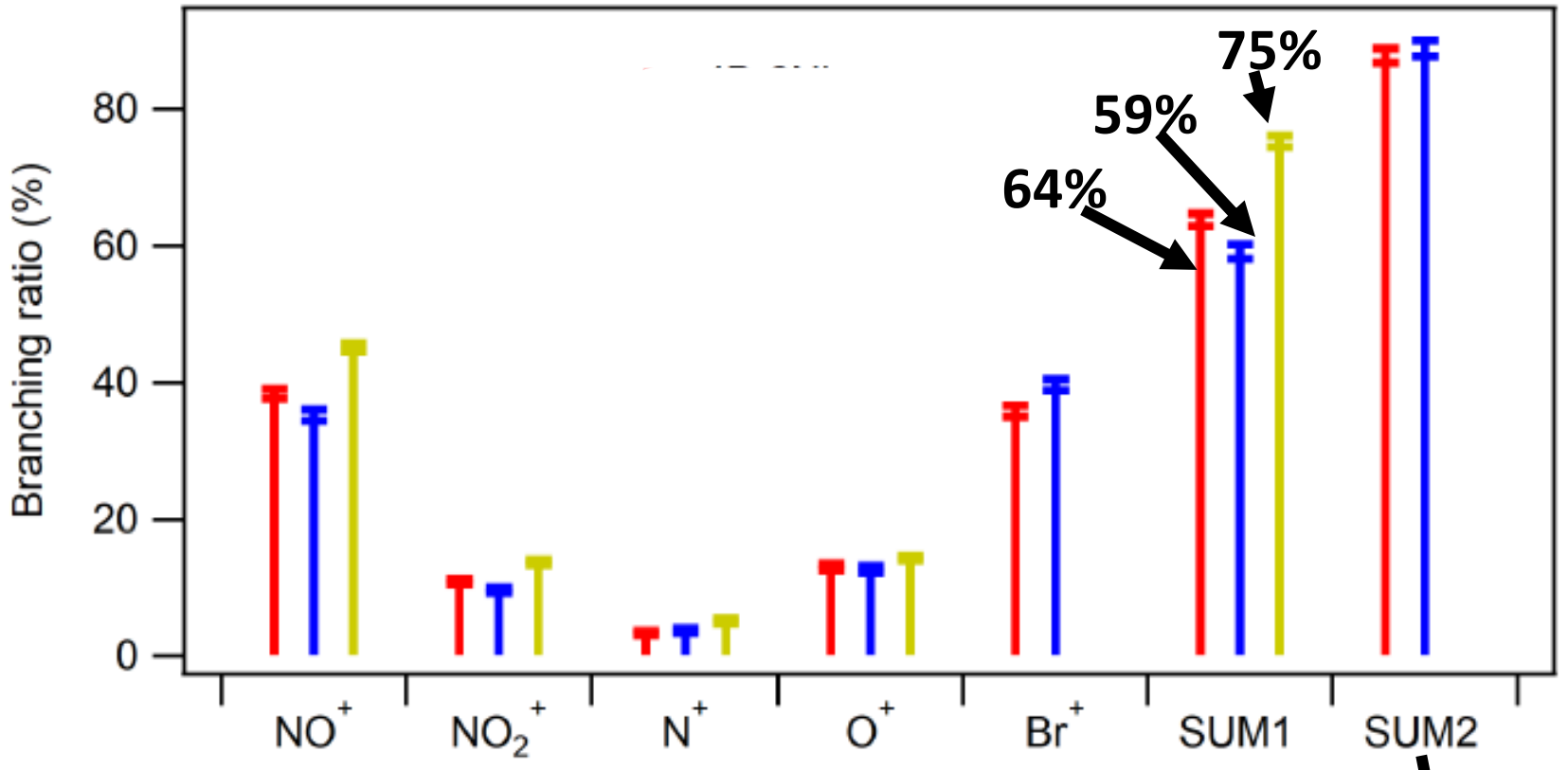

SUM1 + Br^+

NO^+, NO_2^+, N^+, and O^+

MAX IV, FinEstBeAMS

Photofragmentation study №2: iodinated nitroimidazole

Shallow inner-shell vs. deeper inner-shell ionization of high-Z element

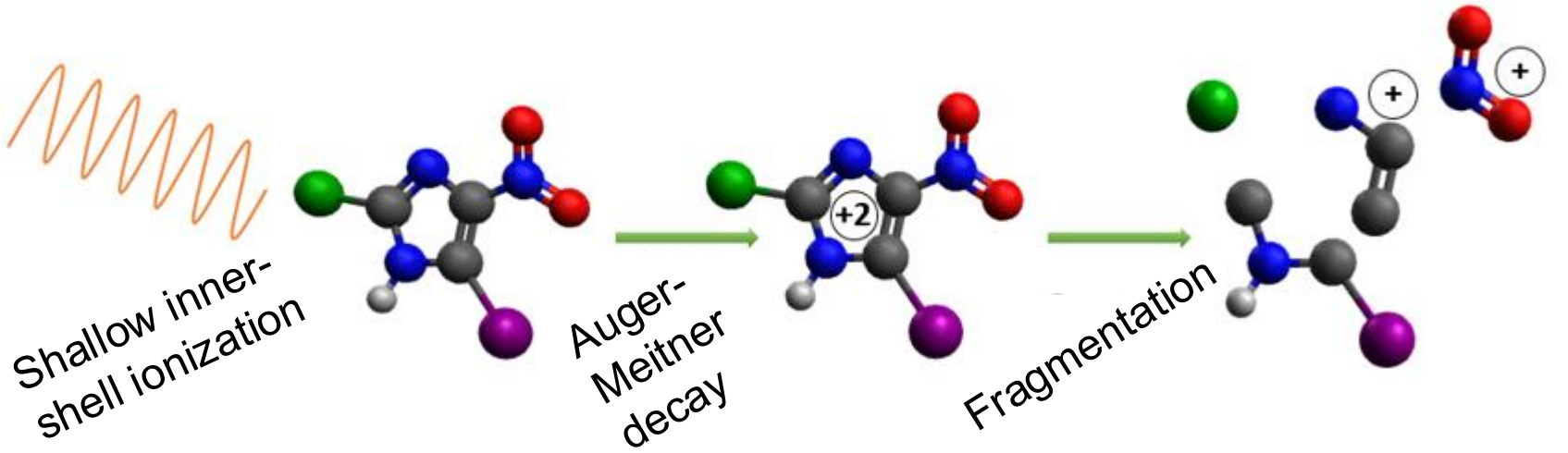

I 4d
hv = 85 eV

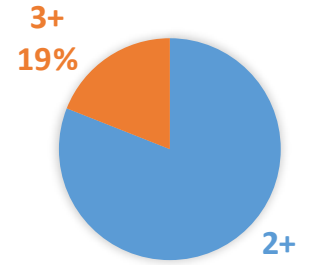

Br 3d
hv = 115 eV

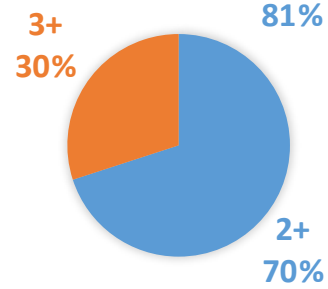

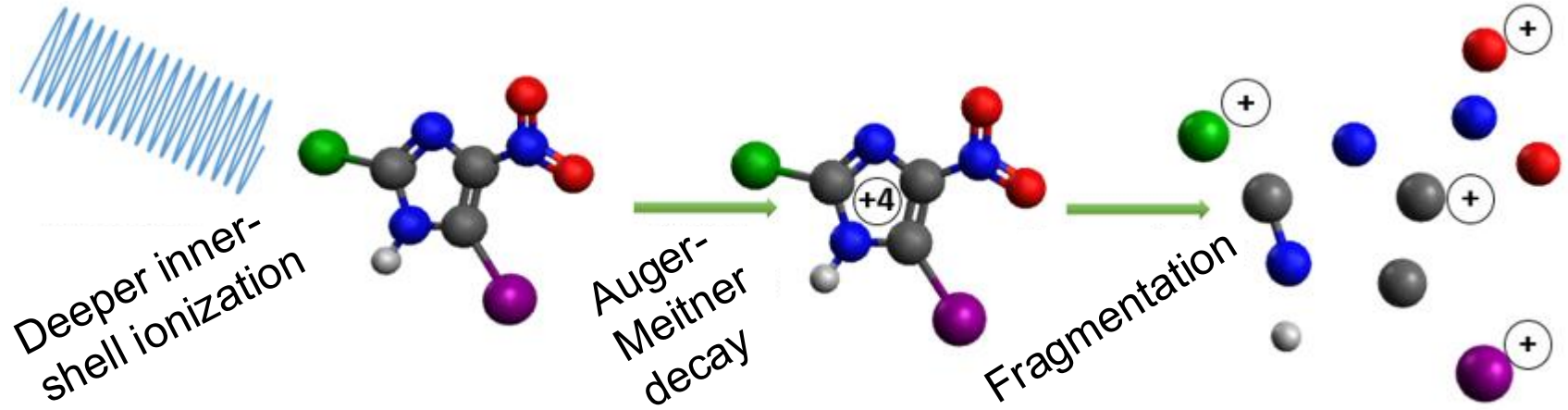

I 3d
hv = 670 eV

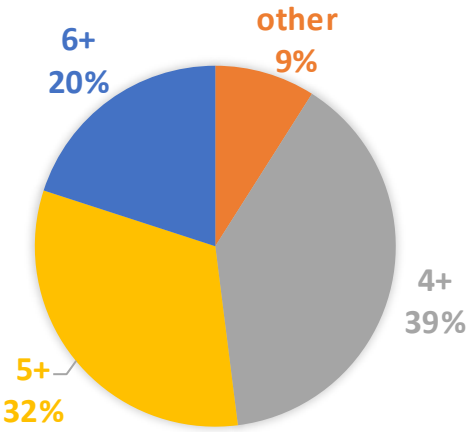

Bar plots from mass spectra measured in coincidence with I 4d, Br 3d, and I 3d photoelectrons

Going from shallow to deeper inner shell:

- The ion distribution shifts toward lighter masses mostly at the expense of **NO^+, NO_2^+, C_2N^+** ions
- More energetic atomic fragments are produced (**C^+, N^+, O^+, I^+, Br^+**)

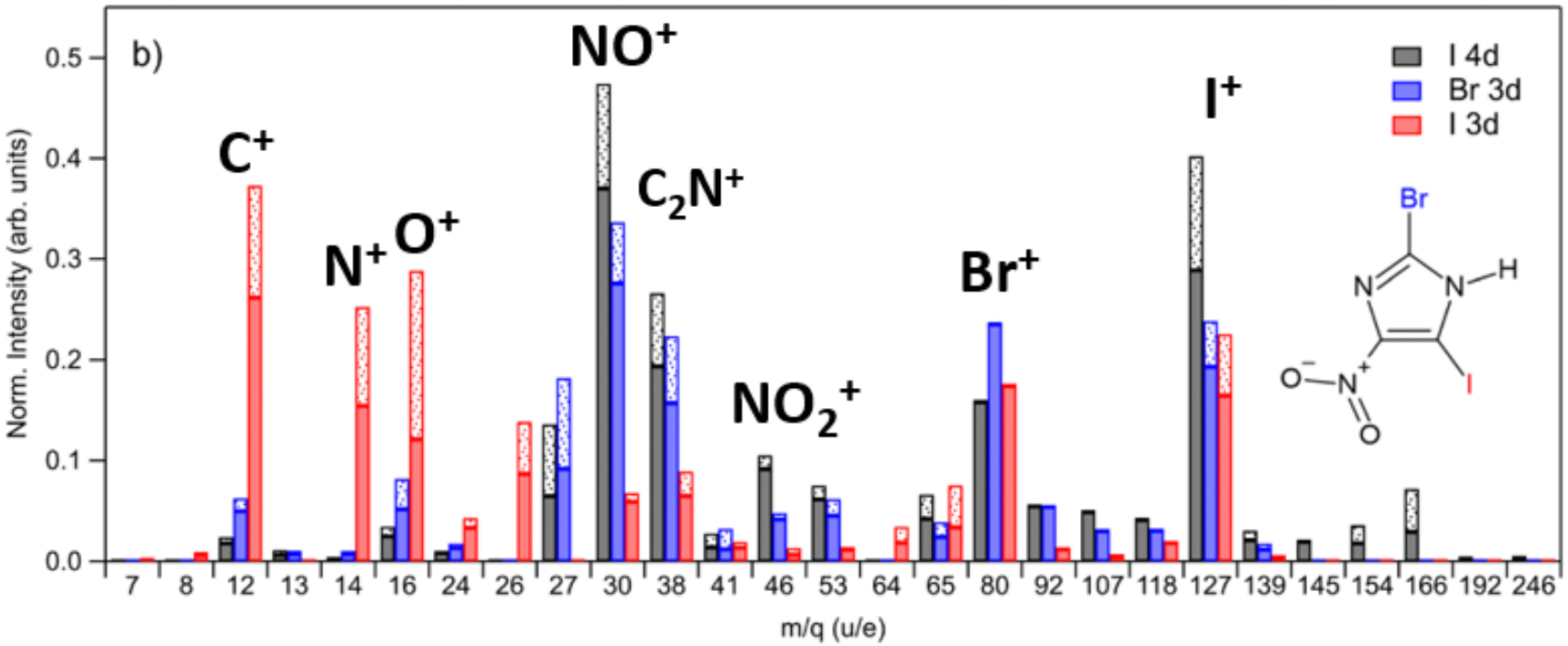

Pihlava L., Svensson P.H.W., Berholts M., et al., *Shell-dependent photofragmentation dynamics of a heavy-atom-containing bifunctional nitroimidazole radiosensitizer,* PCCP, 2024, **26**, 8879-8890

MAX IV, FinEstBeAMS

Experimental kinetic energies of the ions measured in coincidence with I 4d, Br 3d, and I 3d electrons

	I 4d		Br 3d		I 3d	
Ion	E_k	FWHM	E_k	FWHM	E_k	FWHM
N^{++}	—	—	—	—	5.02	1.41
O^{++}	—	—	—	—	1.73	0.55
C^+	1.19	1.02	1.54	1.34	3.07	1.48
CH^+	1.08	0.82	1.23	1.09	—	—
N^+	1.68	1.40	2.25	1.39	5.85	2.95
O^+	2.90	0.81	3.45	0.99	7.96	1.66
C_2^+	1.34	0.94	1.58	1.29	2.63	1.11
CN^+	—	—	—	—	3.23	1.46
CHN^+	1.61	1.15	1.66	1.39	—	—
NO^+	2.59	0.61	2.77	0.83	3.90	1.43
C_2N^+	1.21	1.27	1.26	1.47	2.21	1.80
CHN_2^+	1.97	2.03	2.38	2.51	2.99	1.10
NO_2^+	2.66	0.39	2.65	0.68	3.59	1.95
$C_2HN_2^+$	1.87	1.44	2.01	1.87	2.53	1.51
$C_3N_2^+$	—	—	—	—	2.30	1.26
$C_3HN_2^+$	0.54	0.91	0.40	1.48	2.10	1.79
I^+	1.67	0.57	1.79	0.92	3.30	0.73
CI^+	0.88	0.95	1.09	1.70	—	—
$CHIN^+$	0.52	0.54	—	—	—	—
C_2HIN^+	0.08	0.17	—	—	—	—

Deep I 2p inner-shell ionization and extreme fragmentation

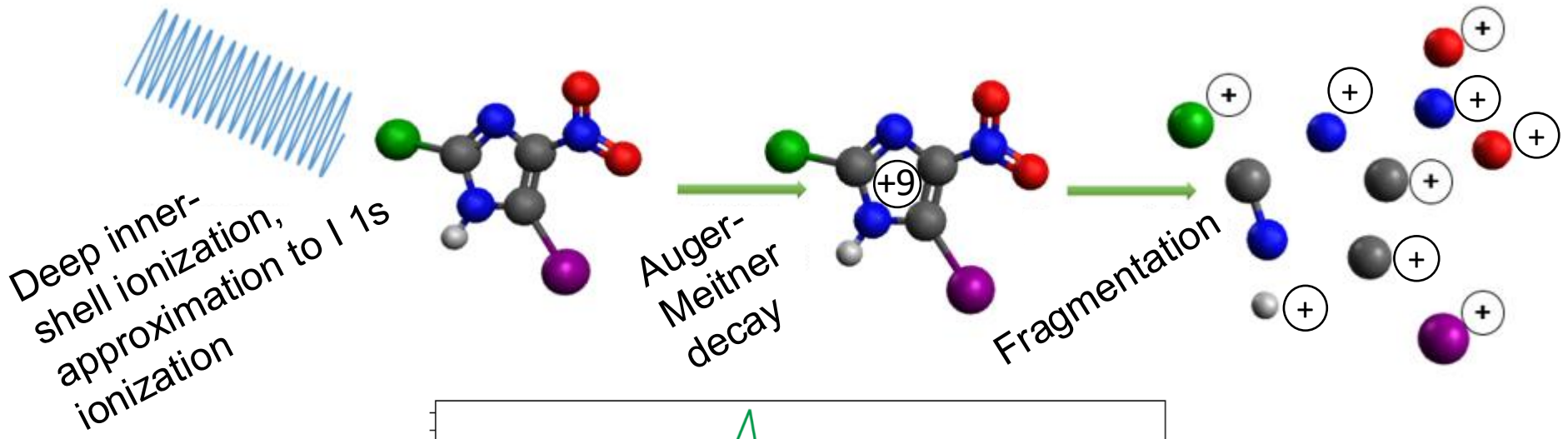

I $2p_{3/2}$ (L_3)
hv = 4665 eV

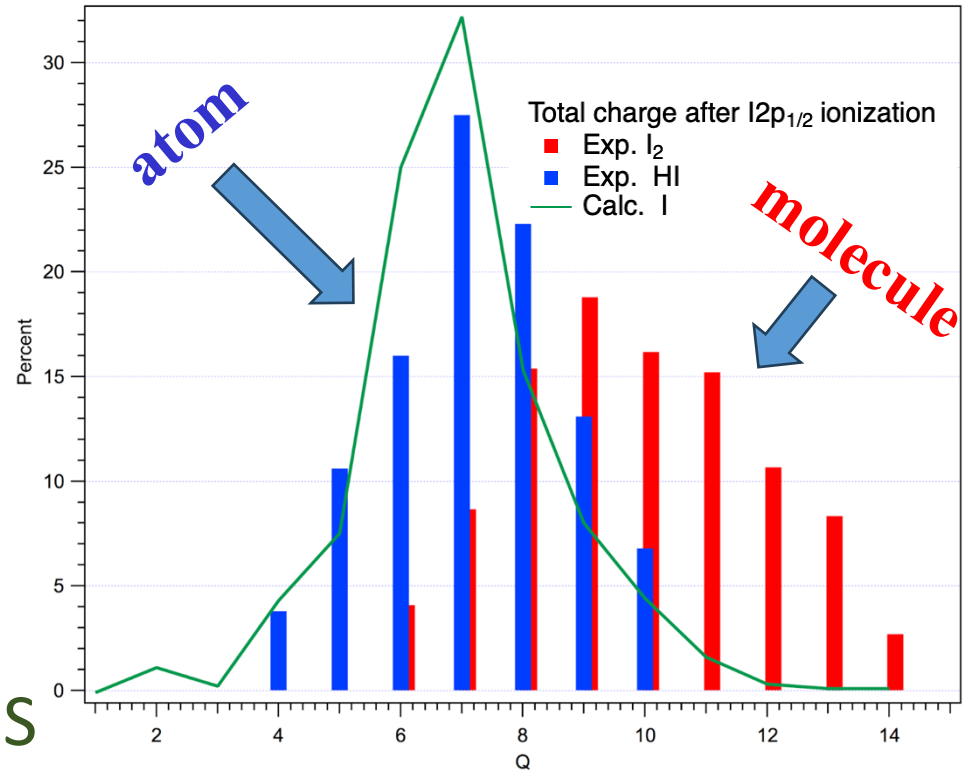

The molecular environment actively fuels the cascade: additional decay steps, higher final charge states, more violent fragmentation

SOLEIL, GALAXIES

Cascades from iodine deep inner shell ionization: K-shell vs. L-shell
How deep is deep enough?

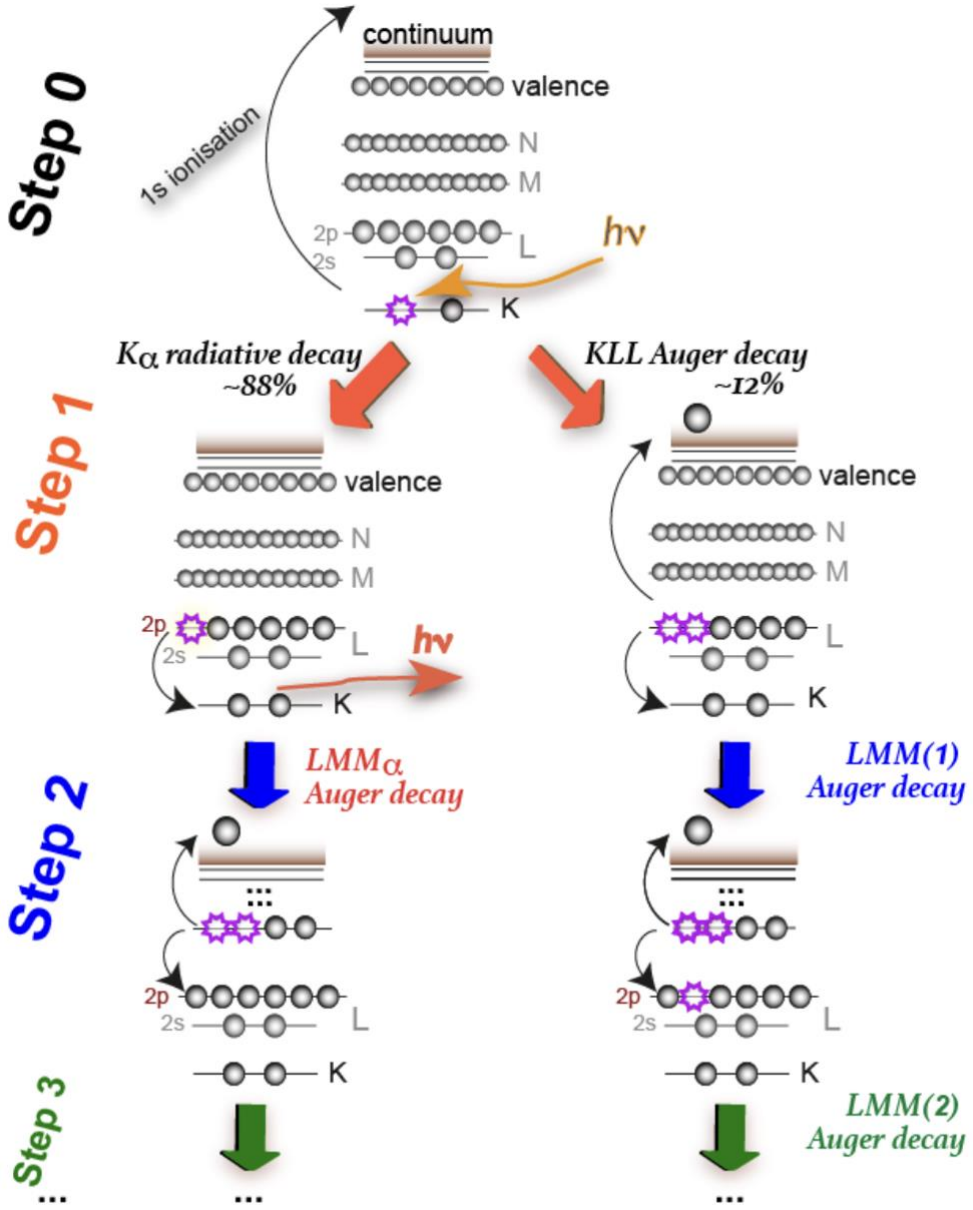

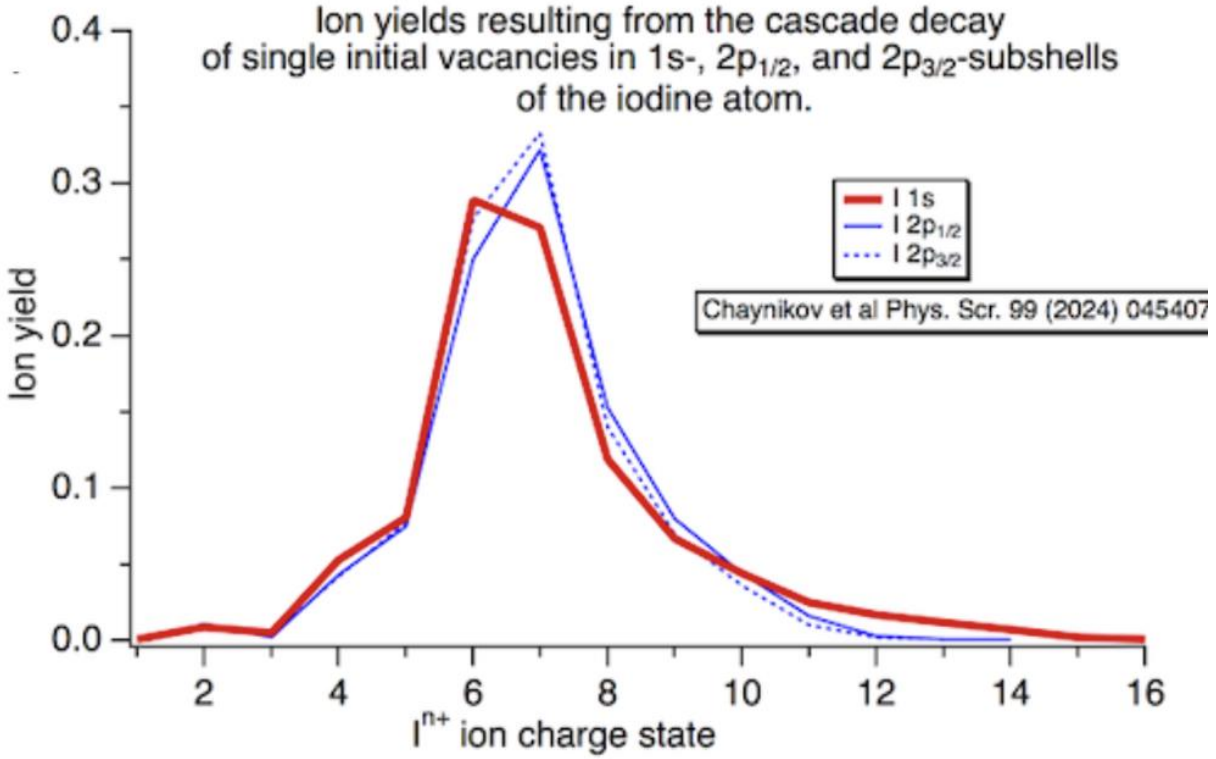

With MUSTACHE, we are now equipped to study medically relevant processes

Conclusions

We can directly observe how radiosensitizers are activated at the molecular level using tools from molecular physics -> mechanistic understanding to move from empirical design toward predictive models for next-generation radiotherapy agents.

Halogenation affects the fragmentation of nitroimidazole radiosensitizers, the effect strongly depends on the incoming photon energy!

- **High-Z atom shallow inner-shell ionization (NO HOTSPOT CONDITIONS):**
  - Similar to non-halogenated RS case, only slightly suppresses the production of nitro group-related fragments (NO^+, NO_2^+) + adds halogen ions
- **High-Z atom deeper inner-shell ionization (HOTSPOT CONDITIONS):**
  - Complete atomization + multiply charged ions => larger number of energetic radiation damage missiles (ions + electrons)

Acknowledgements

Tartu University

- Kuno Kooser
- Arvo Tõnisoo
- Tanel Käämbre

MAX IV

- Antti Kivimäki

Turku University

- Edwin Kukk
- Lassi Pihlava
- Kerttu Pusa
- Johannes Niskanen
- Anton Vladyka

Sorbonne University

- Oksana Travnikova
- Iyas Ismail
- Marc Simon

Uppsala University

- Olle Björneholm
- Pamela H.W. Svensson
- Carl Caleman
- Tomas Andre
- Oscar Grånäs
- Nicusor Timneanu

Funding

Estonian Research Council grant PSG1037


Thank you for your attention!